

Studies on the distribution of acotiamide to stomach

by

Kazuyoshi Yoshii

At the

Chiba University

2016

The thesis was submitted for the degree of Doctor of Philosophy.

Contents

| | |
|---|----|
| 1. Abbreviations | 4 |
| 2. General introduction | 5 |
| 3. Distribution of acotiamide, an orally active acetylcholinesterase inhibitor, into the <i>myenteric plexus</i> of rat and dog stomachs | 8 |
| 3.1. Introduction | 8 |
| 3.2. Materials and Methods | 9 |
| 3.2.1. Chemicals..... | 9 |
| 3.2.2. Animals..... | 9 |
| 3.2.3. AChE staining of rat stomach | 10 |
| 3.2.4. AChE staining of dog stomach | 11 |
| 3.2.5. Macro-autoradiography of rat stomach..... | 11 |
| 3.2.6. Macro-autoradiography of dog stomach..... | 12 |
| 3.2.7. Nissl Staining and Micro-autoradiography of rat stomach | 13 |
| 3.3. Results and Discussion..... | 13 |
| 3.4. Summary | 20 |
| 4. Mechanism for distribution of acotiamide, a novel gastroprokinetic agent for the treatment of functional dyspepsia, in rat stomach | 22 |
| 4.1. Introduction | 22 |
| 4.2. Materials and methods | 22 |
| 4.2.1. Chemicals..... | 22 |
| 4.2.2. Animals..... | 23 |
| 4.2.3. <i>In vivo</i> infusion study..... | 23 |
| 4.2.4. Kinetic analysis of the <i>in vivo</i> stomach distribution of acotiamide | 24 |
| 4.2.5. <i>In vitro</i> binding study..... | 25 |
| 4.2.6. Determination of binding parameters | 26 |
| 4.2.7. Integration plot analysis | 27 |
| 4.2.8. Determination of the stomach-to-plasma unbound concentration ratio of acotiamide | 29 |
| 4.2.9. Quantification of acotiamide by LC-MS/MS | 30 |
| 4.3. Results | 31 |
| 4.3.1. Distribution of acotiamide to the stomach and skeletal muscle in rats..... | 31 |
| 4.3.2. Binding parameters for acotiamide calculated from <i>in vivo</i> infusion study. | 32 |
| 4.3.3. Plasma and stomach tissue protein binding of acotiamide | 33 |
| 4.3.4. Integration plot analysis | 34 |
| 4.3.5. Unbound concentration ratio of stomach to plasma | 36 |

| | | |
|--------|---|----|
| 4.4. | Discussion | 37 |
| 4.5. | Summary | 41 |
| 5. | Physiologically-based pharmacokinetic and pharmacodynamic modeling for the inhibition of acetylcholinesterase by acotiamide, a novel gastroprokinetic agent for the treatment of functional dyspepsia, in rat stomach | 42 |
| 5.1. | Introduction | 42 |
| 5.2. | Materials and Methods | 43 |
| 5.2.1. | Chemicals..... | 43 |
| 5.2.2. | Animals..... | 43 |
| 5.2.3. | Preparation of stomach homogenate for <i>in vitro</i> study..... | 44 |
| 5.2.4. | AChE activity by stomach homogenate..... | 44 |
| 5.2.5. | <i>In vivo</i> study..... | 45 |
| 5.2.6. | Quantification of acotiamide by LC-MS/MS | 46 |
| 5.2.7. | Quantification of ACh by LC-MS/MS | 46 |
| 5.2.8. | PBPK/PD model | 47 |
| 5.3. | Results | 50 |
| 5.3.1. | PBPK modeling | 50 |
| 5.3.2. | Analysis of blood and stomach concentrations of acotiamide..... | 51 |
| 5.3.3. | Inhibition of the hydrolysis of MATP+ by acotiamide..... | 53 |
| 5.3.4. | PD modeling | 53 |
| 5.3.5. | Analysis of stomach concentration of ACh | 54 |
| 5.4. | Discussion | 55 |
| 5.5. | Summary | 59 |
| 6. | Conclusion..... | 60 |
| 7. | References | 63 |
| 8. | Papers in publication | 71 |
| 9. | Acknowledgements | 72 |
| 10. | Reviewers | 74 |

Tables

| | | |
|------------|---|----|
| Table 2-1. | The binding parameters of acotiamide, free fractions in plasma and stomach tissue, and stomach tissue-to-plasma concentration ratio | 33 |
| Table 2-2. | The unbound concentration ratio of stomach to plasma ($C_{st,u,cyt}/C_{p,u}$) after the constant-rate infusion of acotiamide at a dose of 2 nmol/min/kg to rats | 37 |
| Table 3-1. | Physiological and pharmacokinetic parameters for PBPK analysis in rats | 52 |

| | |
|--|----|
| Table 3-2. Fitting quality of the PBPK model for the time course of acotiamide concentrations in blood and stomach | 52 |
|--|----|

Figures

| | |
|---|----|
| Fig. 1. Structure of acotiamide hydrochloride..... | 7 |
| Fig. 1-1. Photomicrograph of AChE activity staining for the muscular layer of rat stomach..... | 14 |
| Fig. 1-2. Photomicrograph of AChE activity staining for the muscular layer of dog stomach..... | 15 |
| Fig. 1-3. Macro-autoradiogram of rat stomach. | 16 |
| Fig. 1-4. Macro-autoradiogram of dog stomach..... | 17 |
| Fig. 1-5. Nissl-stained photomicrograph (A) and micro-autoradiogram (B) of the rat stomach..... | 18 |
| Fig. 2-1. Tissue-to-plasma concentration ratio (K_p) versus plasma concentration in rat stomach and skeletal muscle 120 min after starting constant-rate infusion of acotiamide..... | 32 |
| Fig. 2-2. Protein binding of acotiamide by plasma (A) and stomach tissue (B). | 33 |
| Fig. 2-3. Integration plots representing acotiamide uptake by each examined tissue..... | 35 |
| Fig. 2-4. $f_{u,b} \cdot PS_{inf,app}$ for acotiamide in various tissues after intravenous bolus administration. | 36 |
| Fig. 3-1. Physiologically-based pharmacokinetic and pharmacodynamic model to describe the distribution of acotiamide and AChE inhibition in rat stomach following intravenous administration..... | 48 |
| Fig. 3-2. Profiles and model simulations of acotiamide concentrations in the blood, stomach, precursor pool, and deep pool after intravenous administration to rats. | 51 |
| Fig. 3-3. Inhibition of MATP+ hydrolysis by acotiamide..... | 53 |
| Fig. 3-4. Profile and model simulation of ACh concentration in the stomach homogenate after intravenous administration of acotiamide to rats..... | 54 |

1. Abbreviations

| | |
|----------------|---|
| ACh | Acetylcholine |
| AChE | Acetylcholinesterase |
| AIC | Akaike's information criterion |
| ATCh | Acetylthiocholine |
| AUC | Area under the concentration-time curve |
| BChE | Butyrylcholinesterase |
| B_{max} | Binding capacity |
| C_b | Bound concentration |
| C_f | Unbound concentration |
| $CL_{inf,app}$ | Initial uptake clearance |
| CL_{tot} | Total body clearance |
| FD | Functional dyspepsia |
| f_u | Unbound fraction |
| GFR | Glomerular filtration rate |
| GI | Gastrointestinal |
| IC_{50} | Half maximal inhibitory concentrations |
| K_d | Dissociation constant |
| K_p | Tissue-to-plasma concentration ratio |
| LC-MS/MS | Liquid chromatography-mass spectrometry/mass spectrometry |
| Loglik | Maximized log-likelihood function |
| PBPK | Physiologically based pharmacokinetic |
| PBPK/PD | Physiologically based pharmacokinetic and pharmacodynamic |
| PD | Pharmacodynamic |
| PK | Pharmacokinetic |
| Q_t | Blood flow rate |
| PS | Permeability surface area product |
| R_{bp} | Blood-to-plasma concentration ratio |
| RNA | Ribonucleic acid |
| S.D. | Standard deviation |
| S.E. | Standard error |
| UGT | Uridine 5'-diphosphate glucuronosyltransferase |
| V_d | Distribution volume |

2. General introduction

Functional dyspepsia (FD) is a common gastrointestinal disorder defined as symptom-based conditions in the absence of organic disease [1,2,3]. Symptoms are categorized as postprandial distress and epigastric pain syndromes, which are associated with impaired gastric accommodation and emptying [4,5]. Gastric accommodation and emptying are induced by coordinating motility of gastric fundus, body and antrum, which are regulated by complex nervous systems including cholinergic neurons projected from dorsal motor nucleus of the vagus to the stomach [6,7]. The cholinergic system is regulated by factors such as acetylcholine (ACh). ACh is released from presynaptic neurons into the synaptic cleft, where it then binds to ACh receptors and either affects gastric motility or is inactivated by acetylcholinesterase (AChE). This relationship suggests that gastric motility might be regulated via the inhibition of AChE activity and that AChE inhibitors might effectively treat patients with FD [8,9].

Acotiamide is an AChE inhibitor and first-in-class drug for the treatment of FD [10,11,12,13,14]. Although some clinical studies have suggested that proton pump inhibitors (e.g., omeprazole) and prokinetics (e.g., itopride or mosapride) are effective, no product except for acotiamide has gotten marketing approval for the treatment of patients with FD [10]. Clinical studies have shown that acotiamide enhances the gastric accommodation reflex and gastric emptying rate [11] and improves meal-related symptoms such as postprandial fullness, upper abdominal bloating and early satiation in patients of FD [12]. In rats and dogs, acotiamide enhances gastric emptying and also increases gastrointestinal (GI) motility [15,16], and is expected to inhibit AChE in gastric muscle. Acotiamide is also anticipated to be effective by the distribution from blood to the stomach because acotiamide stimulated gastric motility after both intravenous and oral

administration to dogs [15]. On the other hand some experiments were performed after the subcutaneous administration of acotiamide to rats to investigate the enhancement of gastric motility by acotiamide in detail because the exposure after the subcutaneous administration of acotiamide is higher than that after the oral administration of acotiamide in rats [17]. These experiments suggested that acotiamide in the stomach tissue might be effective for enhancement of gastric motility as the whole stomach tissue concentration of acotiamide was higher than the half maximal inhibitory concentrations (IC_{50}) for AChE after the subcutaneous administration of acotiamide to rats although further studies are needed to determine the concentration of acotiamide around target of its action like AChE [17]. Since the stomach tissue concentration of acotiamide could be important for the pharmacological action of acotiamide, understanding the distribution of acotiamide to target organ is of importance for evaluating the potential of this drug for treating FD.

AChE inhibitors are also used for the treatment of myasthenia gravis as ACh is required for the contraction of muscle fibers [18]. Therefore, the potential adverse effect of acotiamide on skeletal muscle would be an undesirable outcome during the treatment of FD. As cholinergic nerves develop not only in the GI tract, but also in brain tissue, drugs inhibiting AChE would also act on the brain if they passed through the blood-brain barrier. Since distribution into these tissues might cause adverse effects, such as muscle twitching and cholinergic crisis, investigating the distribution of acotiamide to nontarget organs is of importance for estimating the possibility of adverse effects of this drug.

Distribution of drugs to stomach is determined by its physicochemical properties such as solubility, partition coefficient and ionization constant, tissue binding to cellular components, and transport. Especially, pharmacokinetic data related to the transport of drugs from lumen or vessels to the stomach is of considerable interest to gastroenterology researchers. A recent report has provided valuable information for the transfer of

amoxicillin *in vivo* from blood to the stomach in rats, although the main aim of the study was not to investigate the distribution mechanism of this antibiotic [19]. The inhomogeneous mucosal distribution of amoxicillin, whose concentrations in the glandular stomach mucosa were higher than those in the forestomach mucosa, may imply a specific distribution mechanism of the drug. Although *in vitro* uptake studies with isolated cells are a useful technique to identify the possible molecular mechanisms involved in the distribution of a target drug, it is impossible to eliminate the introduction of artifacts or determine if the test compound is transported via basolateral membranes using such *in vitro* approaches. Therefore, further *in vivo* studies using a pharmacokinetic approach are needed for investigating the distribution of acotiamide to the stomach.

Here, the purposes of the present studies were to examine whether the concentration of acotiamide at the site of action is sufficient to inhibit AChE in chapter 1, to reveal the mechanism of distribution of acotiamide to stomach in chapter 2, and to elucidate a role of distribution of acotiamide in the pharmacokinetics and pharmacodynamics of acotiamide in chapter 3.

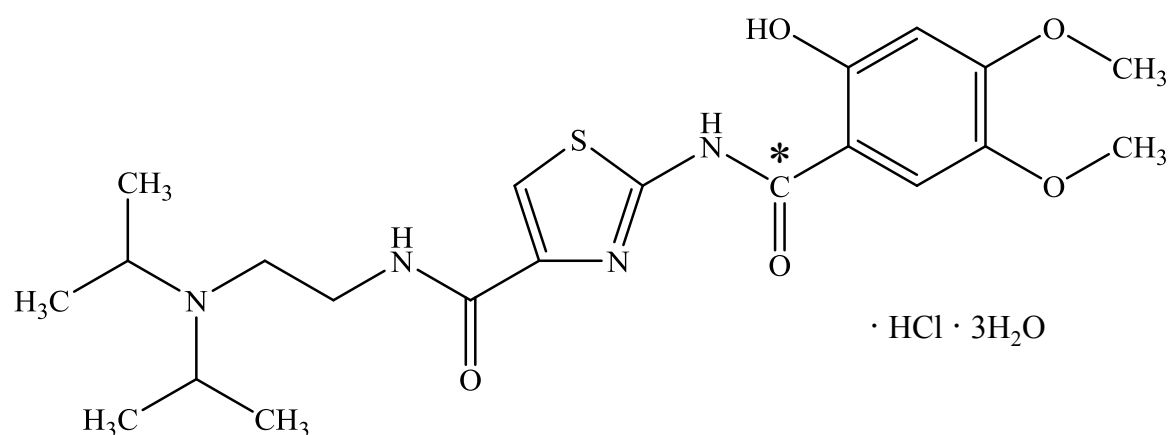


Fig. 1. Structure of acotiamide hydrochloride.

3. Distribution of acotiamide, an orally active acetylcholinesterase inhibitor, into the *myenteric plexus* of rat and dog stomachs

3.1. Introduction

The pharmacological and therapeutic effects of acotiamide are thought to be derived from its inhibitory effects on acetylcholinesterase (AChE) which results in the potentiation cholinergic neurons [15]. In fact, an *in vitro* animal experiment showed that acotiamide enhanced acetylcholine (ACh)-induced but not carbachol (not hydrolyzed by AChE)-induced contraction of isolated gastric antrum strips of guinea pig [15]. In addition, an *in vivo* animal experiment showed that acotiamide enhanced gastric body contractions induced by electrical stimulation of the vagus nerve in rats, which were completely abolished by classical antagonist of ACh receptors [17].

Acotiamide inhibits AChE with half maximal inhibitory concentrations (IC_{50}) of 3.0, 2.3 and 1.2 μ M for human recombinant, and rat and canine gastric AChEs, respectively [15,17]. These values are much larger than those of classical inhibitors of AChE, such as neostigmine, however, acotiamide is concentrated into the stomach tissue by carrier-mediated uptake processes, which may account for the selective action of acotiamide for gastric smooth muscle but not for skeletal muscle and central nervous system in rats [20].

Myenteric plexus is a mesh-like system of neurons which provide major motor innervation to the gastrointestinal muscles [21]. Therefore, main target of acotiamide action is thought to be AChE localized around the cholinergic nerve terminals in the *myenteric plexus* which is located in the muscular layer of the stomach. However, whether sufficient concentrations of acotiamide are attained in the *myenteric plexus* of the stomach to inhibit AChE, has not been confirmed in any species yet, although the total

concentrations of acotiamide in the homogenate of rat stomach after *in vivo* administration were reported to be higher than *in vitro* IC₅₀ value of acotiamide estimated from rat gastric AChE [17].

The aim of the present study was to examine the distribution of acotiamide into the *myenteric plexus* of the stomach after [¹⁴C]acotiamide dose enough to exhibit pharmacological action, using macro- and micro-autoradiographs, and to estimate whether the sufficient concentration of acotiamide is attained in the *myenteric plexus* of the stomach, a putative site of acotiamide action, to inhibit AChE in rat and dog stomachs.

3.2. Materials and Methods

3.2.1. Chemicals

N-[2-[bis(1-methylethyl)amino]ethyl]-2-[(2-hydroxy-4,5-dimethoxybenzoyl)amino]thiazole-4-carboxamide monohydrochloride trihydrate (acotiamide hydrochloride, Z-338/YM443) was synthesized in the central research laboratories of Zeria Pharmaceutical Co., Ltd. (Saitama, Japan). [¹⁴C]Acotiamide (2.26 GBq/mmol) was synthesized by GE Healthcare UK Ltd. (Buckinghamshire, England). All other chemicals were of reagent grade.

3.2.2. Animals

Male Sprague-Dawley rats aged six to seven weeks were obtained from Charles River Japan, Inc. (Kanagawa, Japan) and housed under standard controlled environmental conditions at 23 ± 3°C and 55 ± 20% humidity with a 12-h light/dark cycle, and food (CRF-1; Oriental Yeast Co., Ltd., Tokyo, Japan or CE-2; CLEA Japan Inc., Tokyo, Japan) and water available *ad libitum*. Rats were allowed to acclimate to laboratory conditions for at least one week prior to experiments.

Male beagle dogs were obtained from Oriental Yeast Co., Ltd. (Tokyo, Japan) or the Institute for Animal Reproduction (Ibaraki, Japan) and housed individually in experimental cages where they were acclimated for at least 12 days before entry to the study. Laboratory chow (NVE-10, Nihon Pet Food K.K., Tokyo, Japan; or DS-A, Oriental Yeast Co., Ltd.) was provided once daily and water was given *ad libitum*. Animals were housed under standard controlled environmental conditions at $22 \pm 3^{\circ}\text{C}$ and $50 \pm 20\%$ humidity with a 12-h light/dark cycle.

All animal experiments were approved by the Animal Care and Use Committee of the Central Research Laboratories of Zeria Pharmaceutical Co., Ltd., Animal Ethical Committee, Tsukuba Laboratories, Nemoto Science Co., Ltd. (Ibaraki, Japan) and the Institutional Animal Care and Use Committee of Shin Nippon Biomedical Laboratories, Ltd. (Wakayama, Japan).

3.2.3. AChE staining of rat stomach

Rats were exsanguinated *via* the abdominal aorta under anesthesia with diethyl ether and the stomach was excised, washed with saline, ligated at the pylorus, filled with OCT compound through the cardia, ligated at the cardia. Stomach was embedded with OCT compound and frozen in a bath of isopentane and dry ice. Embedded stomach was cut into 6- μm -thick sections using a cryomacrocut CM1900, and immersed in 3 mM copper sulfate/0.05 mM potassium ferricyanide solution containing acetylthiocholine iodide at 37°C for 90 min. After rinsing in distilled water, sections were immersed in Mayer's hematoxylin for 10 min and then washed with running tap water, dehydrated in ethyl alcohol, and immersed in xylene.

3.2.4. AChE staining of dog stomach

Dogs were euthanized by intravenous administration of sodium pentobarbital and supersaturated potassium chloride solutions. Stomach was immediately excised, and divided into 2 pieces along the greater curvature. The pieces were rinsed with physiological saline and divided into approximately 1.5 cm × 1.5 cm sections and frozen in liquid nitrogen. Sections were embedded with an OCT compound and frozen in hexane and dry ice. The frozen serial sections were prepared as 8- μ m sections using a cryomacrocut CM1900. The sections were immersed as described in AChE staining of stomachs of rats.

3.2.5. Macro-autoradiography of rat stomach

As any pharmacological effects haven't been reported after oral administration of acotiamide to rats although acotiamide is orally administered for the treatment of FD, rats were subcutaneously administered with [¹⁴C]acotiamide (30 mg and 20.6 MBq/kg). These dose and route of acotiamide administration were reported to increase the gastric motility index significantly until 90 min after the administration to rats [17]. Rats were exsanguinated via the abdominal aorta under anesthesia with diethyl ether, and the stomach was excised at 30 min after the administration of acotiamide. The excised stomach was washed with saline, ligated at the pylorus, filled with 2% CMC-Na through the cardia, ligated at the cardia, embedded with 2% CMC-Na and frozen in a hexane/dry ice bath. The embedded stomach was cut into 40- μ m-thick sections using a cryomicrotome CM3600 (Leica Microsystems GmbH, Wetzlar, Germany). Sections were exposed by contact with an Imaging-Plate BAS-III2040 (Fuji Photo Film, Tokyo, Japan) in a shield box for 16 h. After exposure, the Imaging-Plate was analyzed with a Bio-Imaging Analyzer BAS-2000 (Fuji Photo Film, Tokyo, Japan) to obtain

macro-autoradioluminograms and measure radioactivities in the tissues. The concentration of the radioactivity in the tissue was quantified by the absolute calibration method [22,23,24,25]. The calibration curve through the origin ($Y=aX$) was prepared based on the mean value of the intensity of luminescence (PSL-BG/mm²) of the blood simultaneously collected when stomach was removed and blood concentration of acotiamide determined by a liquid scintillation analyzer LSC-6100 (Aloka, Tokyo, Japan). The background (BG) value was calculated as the mean value of the intensity of luminescence in three positions on the rim of the section. The lower limit of quantification was defined as twice the BG value. Tissue concentration of acotiamide (mean \pm standard deviation) was expressed as μ M based on the assumption that tissue specific gravity equals 1 g/ml.

3.2.6. Macro-autoradiography of dog stomach

Dogs were anaesthetized with medetomidine and isoflurane, and subjected to abdominal incision. A catheter was inserted into the duodenum from an incision and [¹⁴C]acotiamide (30 mg and 1 MBq/kg) was administered. These dose and route of acotiamide administration were reported to increase the gastric motility index significantly at least until 30 min after the administration to dogs [26]. Dogs were euthanized by intravenous administration of 64.8 mg/ml sodium pentobarbital solution (2 ml/kg) at 30 min after dosing. The cardia of the stomach was tied with a silk suture and the stomach was promptly enucleated. The excised stomach was washed with saline and ligated at the pylorus. The stomach was embedded with 5% CMC-Na and frozen in a bath of hexane and dry ice. The embedded stomach was cut into 30- μ m-thick sections using a cryomicrotome CM3600, which were exposed by contact with an Imaging-Plate BAS-MS2040 in a shield box for 16 h. After exposure, the Imaging Plate was analyzed with the Bio-Imaging Analyzer BAS-2500 (Fuji Photo Film, Tokyo, Japan) to obtain

macro-autoradioluminograms and measure radioactivities in the tissues. The concentration of the radioactivity in the tissue was quantified by the absolute calibration method as described in macro-autoradiography of rat stomach. Tissue concentration of acotiamide (mean \pm standard deviation) was expressed as μM based on the assumption that tissue specific gravity equals 1 g/ml.

3.2.7. Nissl Staining and Micro-autoradiography of rat stomach

Rats were treated with [^{14}C]acotiamide and the stomach was excised as described in macro-autoradiography of rat stomach. Excised stomach was washed with saline, immersed in 10% formalin, and then placed in gum sucrose solution. Once complete submersion was confirmed, stomach was ligated at the pylorus, filled with OCT compound through the cardia, ligated at the cardia, embedded with an OCT compound and frozen in liquid nitrogen. Serial sections of 6- μm -thick were obtained with a cryomacrocut CM1900 (Leica Microsystems GmbH) and attached onto MAS-coated glass slides (Matsunami Trading Co., Ltd., Osaka, Japan) covered with emulsion for the micro-autography and without emulsion for Nissl staining. For Nissl staining, sections were dehydrated in ethanol, rehydrated in distilled water and submerged in 0.1% cresyl violet solution for approximately 30 min until the desired depth of staining was achieved. Sections were dehydrated in ethanol, immersed in xylene, and covered with a coverslip. For the micro-autoradiography, sections were set in a slide glass case and dried completely, then exposed in a refrigerator at 4°C for 2 weeks. Sections were developed, subjected to hematoxylin and eosin staining, and finally covered with a coverslip.

3.3. Results and Discussion

Although the localization of AChE in the muscular layer of the stomach has been reported for humans [27], little information is available on the experimental animals.

Therefore, we studied the localization of AChE in the muscular layer of rat and dog stomachs using AChE staining. As shown in the Fig. 1-1, AChE-activity was detected around the nerve cells in the muscular layer of the rat stomach, which were located between the circular and longitudinal muscles, indicating that the nerve cells are components of the *myenteric plexus*. Similarly, AChE-activity was also found in the ganglia of the *myenteric plexus* of the dog stomach (Fig. 1-2). These findings are consistent with those of humans [27], and suggest that major target of acotiamide action in rats and dogs is AChE in the ganglia of *myenteric plexus* located in the muscular layer of the stomach.

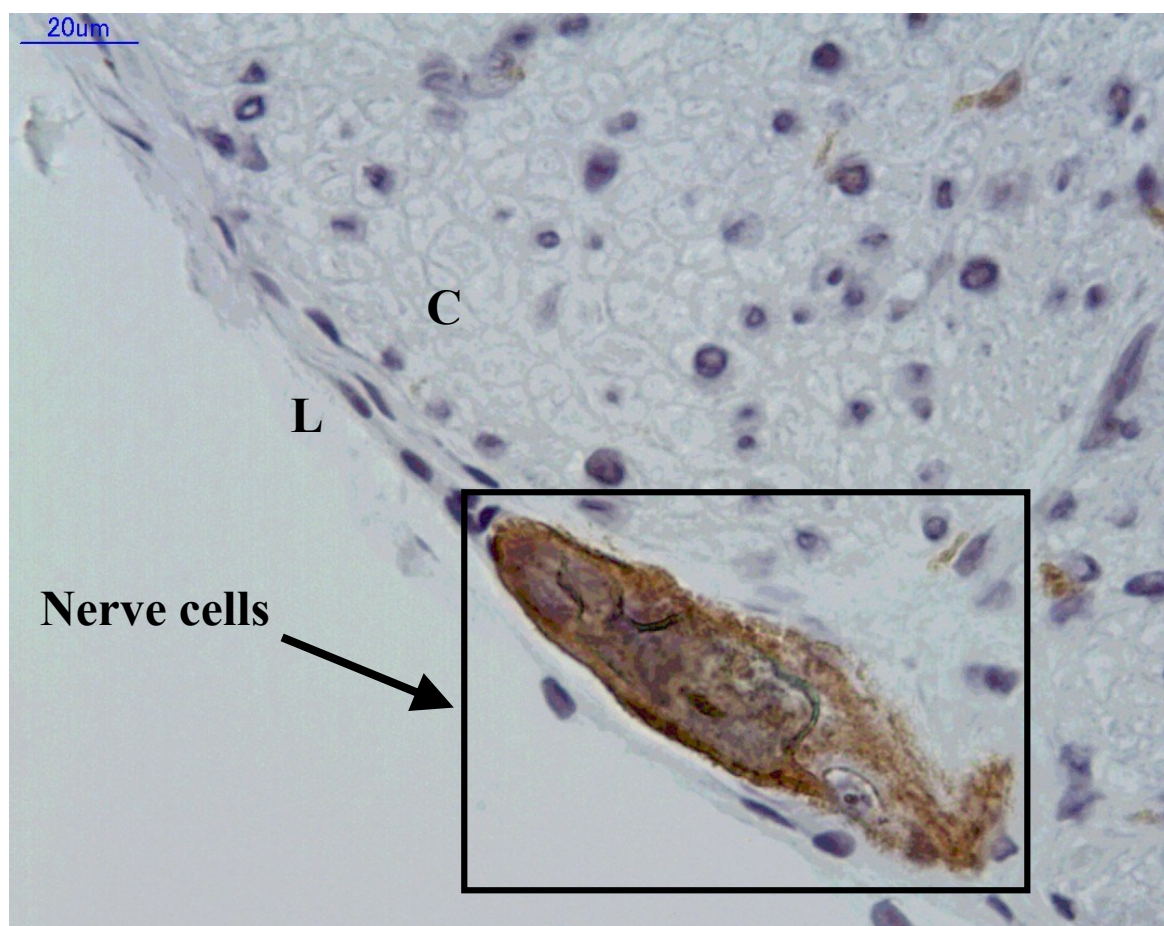


Fig. 1-1. Photomicrograph of AChE activity staining for the muscular layer of rat stomach. The stomach was embedded with OCT compound. Embedded stomach was cut into 6- μm -thick sections and immersed in 3 mM copper sulfate/0.05 mM potassium ferricyanide solution containing

acetylthiocholine iodide at 37°C for 90 min. Then, sections were immersed in Mayer's hematoxylin, dehydrated in ethyl alcohol, and immersed in xylene. Scale bar represents 20 μm . Arrow in photomicrograph indicates nerve cells, and brownish site indicates AChE activity staining located between the circular (C) and longitudinal (L) muscles.

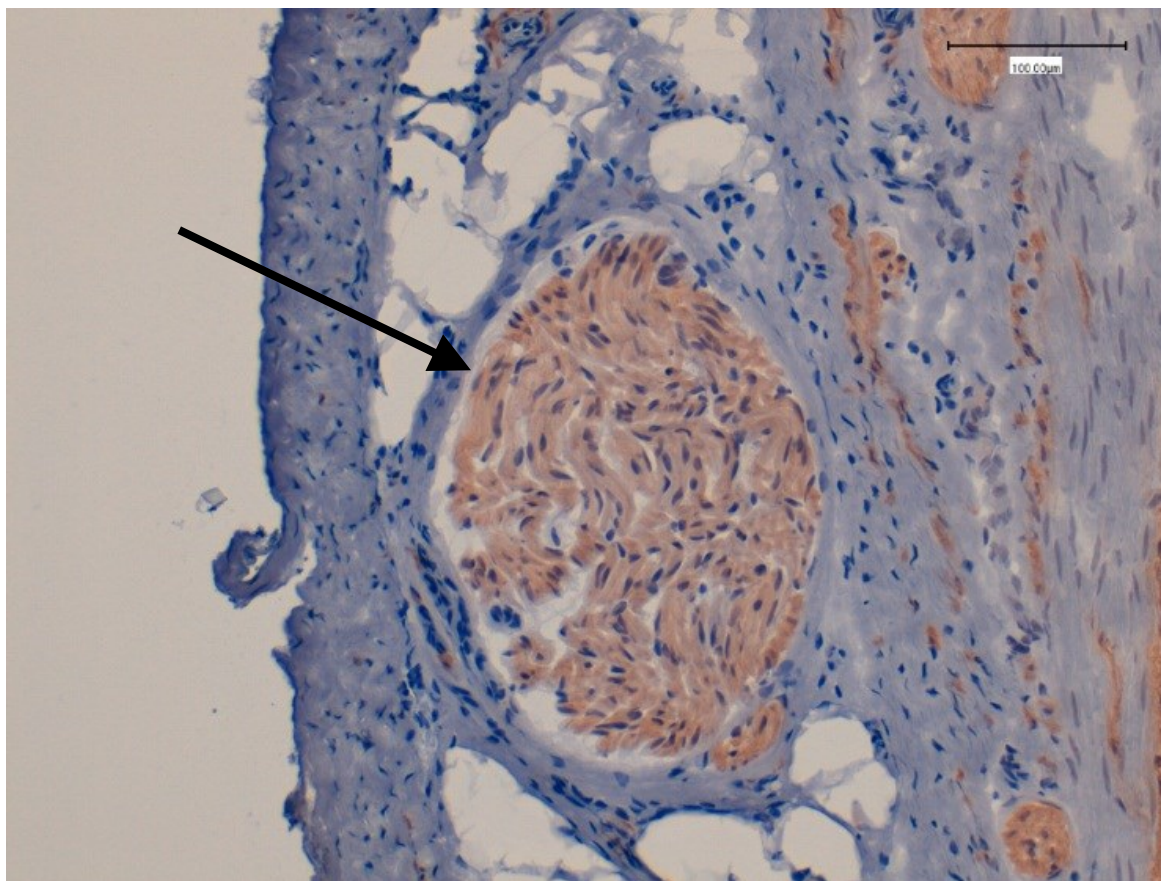


Fig. 1-2. Photomicrograph of AChE activity staining for the muscular layer of dog stomach. The stomach was embedded with OCT compound. Embedded stomach was cut into 8- μm sections and immersed as described in AChE staining of rat stomach. Scale bar represents 100 μm . Arrow in photomicrograph indicates the ganglia, and brownish site indicates AChE activity staining.

Macro-autoradiograms of rat and dog stomachs after the administration of [^{14}C]acotiamide are shown in Fig. 1-3 and Fig. 1-4, respectively. The autoradiograms of rat and dog stomachs showed no marked difference of the radioactivity between the stomach sections. The mean concentration of acotiamide in the stomach of rats estimated from the radioactivity was $27.9 \pm 10.4 \mu\text{M}$ ($n=3$), which was 12 times higher than IC_{50} of acotiamide ($2.3 \mu\text{M}$) estimated from an *in vitro* experiment using rat gastric AChE [17].

Although mucosal and muscular layers were not distinguishable in the rat stomach (Fig. 1-3), they were distinguished in the dog stomach (Fig. 1-4). The mean concentration of radioactivity in the muscular layer of the dog stomach ($1.41 \pm 0.18 \mu\text{M}$, $n=3$) was approximately two-times lower than that of mucosal layer ($3.24 \pm 0.66 \mu\text{M}$, $n=3$), however, it was approximately 1.2 times higher than IC_{50} of acotiamide ($1.2 \mu\text{M}$) estimated from an *in vitro* experiment using dog gastric AChE [15].

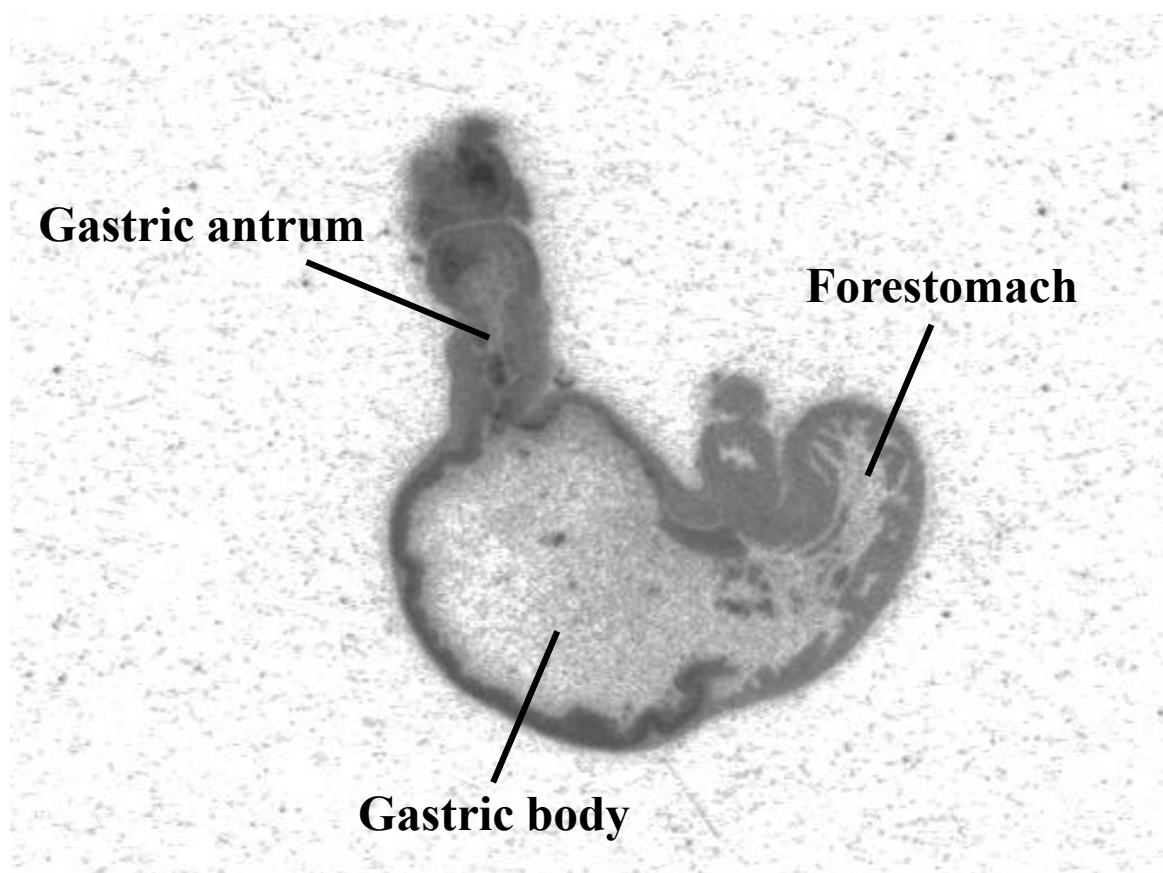


Fig. 1-3. Macro-autoradiogram of rat stomach.

Thirty mg/kg of [^{14}C]acotiamide (20.6 MBq/kg) were administered subcutaneously to rats and the stomach was excised at 30 min after the administration. The excised stomach was embedded with 2% CMC-Na, sliced into 40- μm -thick sections, exposed to imaging plate for 16 h and analyzed with imaging analyzer.

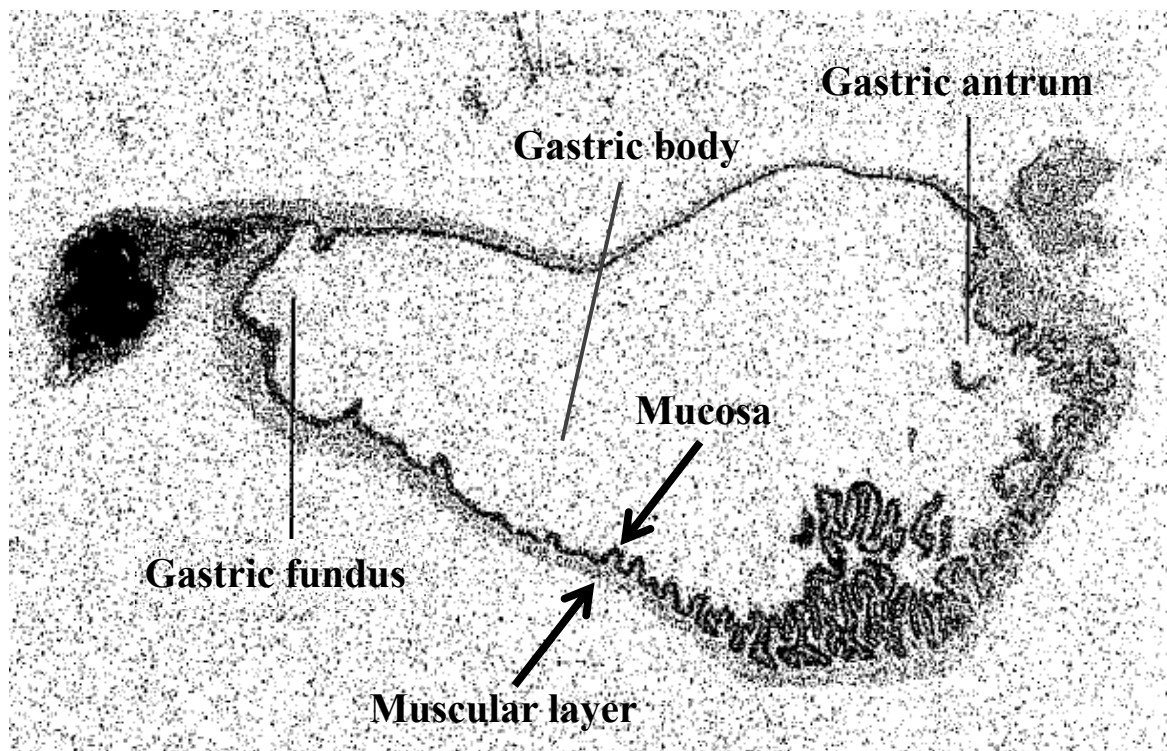


Fig. 1-4. Macro-autoradiogram of dog stomach.

Thirty mg/kg of [^{14}C]acotiamide (1 MBq/kg) were administered intra-duodenally to dogs and the stomach was excised at 30 min after the administration. The stomach was embedded with 5% CMC-Na, sliced into 30- μm -thick sections, exposed to imaging plate for 16 h and analyzed with imaging analyzer.

Nissl stained and micro-autoradiographic images of the muscular layer in the rat stomach are shown in Fig. 1-5A and B, respectively. As shown in the Fig. 1-5A, Nissl stain clearly visualized nerve cells of *myenteric plexus* in the muscular layers of rat stomach. Micro-autoradiogram also showed that the radioactivity distributed homogenously in the muscular layer (the radioactivity was detected as black-silver grains) and distribution of the radioactivity was not apparently different between the surrounding of nerve cells and other regions of muscular layer of rat stomach (Fig. 1-5B). The results suggest that the concentration of radioactivity around the ganglion of the *myenteric plexus* is similar to that in the muscular layer of the rat stomach. However, in the case of rats, the result of the macro-autoradiography showed that the muscular layer could not be

distinguished from mucosal layer (Fig. 1-3) probably due to the thinness of the rat gastric wall. Thus, it may be impossible to estimate the concentrations of radioactivity directly from the macro-autoradiography. Nonetheless, assuming the difference in the concentrations of acotiamide between muscular and mucosal layers found in dog stomach is similar to that in rat stomach, the concentrations of radioactivity in the muscular layer of rat stomach are estimated to be 8.5 μM , which was still much higher than IC_{50} of acotiamide (2.3 μM) estimated from an *in vitro* experiment using rat gastric AChE [17]. On the other hand, in the case of dogs, the concentrations of radioactivity in the muscular layer could be directly estimated from macro-autoradiography, therefore the concentrations of radioactivity around the ganglion of the *myenteric plexus* would be identical to those estimated from macro-autoradiography (1.41 μM). The concentration was higher than IC_{50} of acotiamide for dog gastric AChE (1.2 μM) [15], as described above. These findings suggest that adequate amount of acotiamide could distribute into the ganglion of the *myenteric plexus* of the stomach to inhibit AChE in both of the rat and dog stomachs.

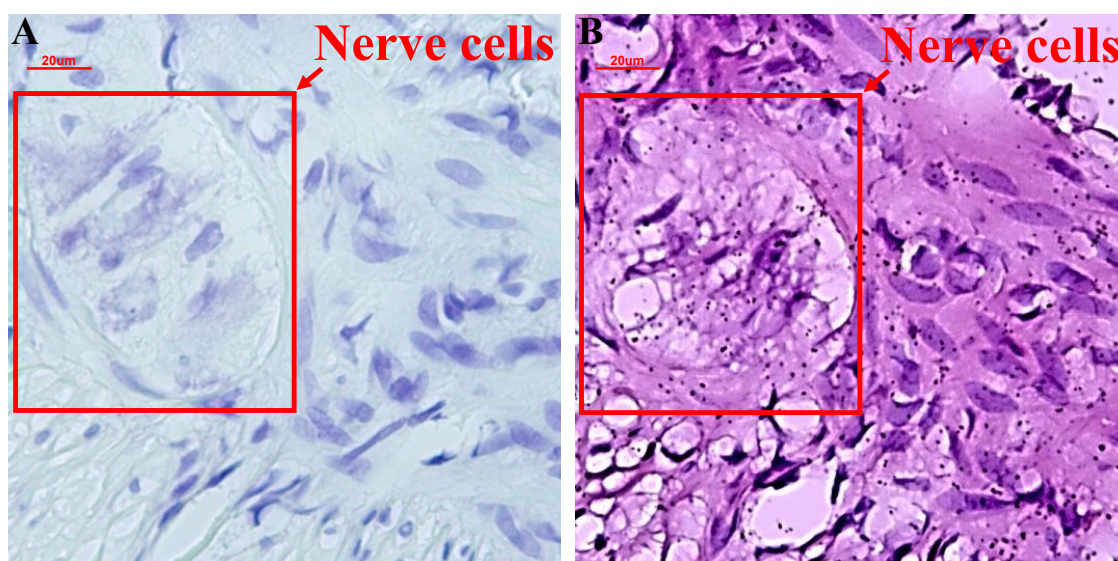


Fig. 1-5. Nissl-stained photomicrograph (A) and micro-autoradiogram (B) of the rat stomach.

Thirty mg/kg of [^{14}C]acotiamide (20.6 MBq/kg) were administered subcutaneously to rats and the stomach was excised at 30 min after the administration. The stomach was embedded with OCT compound. Embedded stomach was cut into 6- μm -thick sections. Serial sections were attached onto glass slides covered with emulsion for the micro-autography and without emulsion for Nissl staining. For Nissl staining, sections were dehydrated in ethanol, rehydrated in distilled water and submerged in 0.1% cresyl violet solution for approximately 30 min. Sections were dehydrated in ethanol, immersed in xylene, and covered with a coverslip. For the micro-autoradiography, sections were dried completely, then exposed in a refrigerator at 4°C for 2 weeks. Sections were developed, subjected to hematoxylin and eosin staining, and finally covered with a coverslip. Scale bars represent 20 μm . The red arrows indicate nerve cells.

Finally, it should be notified that radioactivity is not always identical to acotiamide but can be metabolites of acotiamide or the mixture of acotiamide and its metabolites. Although we do not have direct evidence that radioactivity in the stomach mainly represents unchanged acotiamide, the concentration of acotiamide in the homogenate of rat stomach determined by high performance liquid chromatography reported previously [17] is not so different from the concentration of the radioactivity in the rat stomach found in the present study. Thus, the radioactivity found in the rat stomach is considered to be mainly unchanged acotiamide. In the case of dogs, the concentration of acotiamide in the homogenate of stomach has not been reported. However, plasma concentration-time profiles of acotiamide and radioactive acotiamide after the administration of the same dose of acotiamide as the present study to dogs indicate that plasma concentration of unchanged acotiamide at 30 min (equal to the sampling time of dog stomach in the present study) after the oral administration is almost identical to that of radioactivity at 30 min after the oral administration of the same dose of [^{14}C]acotiamide to dogs (Yoshii et al., unpublished observation). The findings suggest that radioactivity mainly represents unchanged acotiamide at least in plasma at 30 min after the administration of [^{14}C]acotiamide. The findings also suggest that acotiamide is not extensively metabolized at 30 min and

unchanged acotiamide appears to predominantly distribute into the stomach at 30 min after the oral administration to dogs. Thus, the radioactivity found in the dog stomach is also considered to be mainly unchanged acotiamide.

In conclusion, the results of the present study showed that the radioactivity distributes into the *myenteric plexus*, a putative site of acotiamide action, in the muscular layer of the rat and dog stomachs, and that the concentrations of radioactivity around the *myenteric plexus* are estimated to be adequate to inhibit AChE in rats and dogs. Since the dose of acotiamide used in the present study was enough to exhibit pharmacological action in rats and dogs [17,26], the present findings suggest that inhibition of gastric AChE is a major mechanism of action responsible for the pharmacological effects of acotiamide on the gastrointestinal tract of rats and dogs, and may be for the therapeutic effects on the symptoms of patients with FD.

3.4. Summary

Acotiamide is the first-in-class drug for the treatment of functional dyspepsia. Although pharmacological and therapeutic actions of acotiamide are thought to be derived from its inhibitory effects on AChE, whether the concentration of acotiamide at the site of action is sufficient to inhibit AChE remains unclear. Since major site of acotiamide action is thought to be the cholinergic nerve terminals in gastric *myenteric plexus*, we studied the distribution of [¹⁴C]acotiamide into gastric *myenteric plexus*.

Distribution of [¹⁴C]acotiamide was evaluated using macro- and micro-autoradiography in rats and dogs.

The results of macro-autoradiography showed the concentration of radioactivity was 27.9 μ M in rat stomach, which was 12 times higher than IC₅₀ of acotiamide for rat AChE. Being different from rats, the distribution of radioactivity in the muscular layer was

distinguishable from that in the mucosal layer in dog stomach. The concentration of radioactivity in the muscular layer of dog stomach (1.41 μM) was approximately two-times lower than those in the mucosal layer, however, it was approximately 1.2 times higher than IC_{50} of acotiamide for dog AChE. The results of micro-autoradiography also showed the radioactivity distributed homogenously in the muscular layer of rat stomach, suggesting the concentration of radioactivity around the ganglion of *myenteric plexus* is similar to that in the muscular layer of stomach.

These findings suggest acotiamide distributes to the *myenteric plexus* of stomach, a putative site of acotiamide action, with adequate concentrations to inhibit AChE, in both of rat and dog stomachs.

4. Mechanism for distribution of acotiamide, a novel gastroprokinetic agent for the treatment of functional dyspepsia, in rat stomach

4.1. Introduction

Acotiamide is distributed around nerve cells in the *myenteric plexus* of stomach; however, the mechanism of distribution of acotiamide from blood to stomach has not been clarified. To investigate the tissue distribution of acotiamide in rats, the steady state distribution of acotiamide was evaluated in two different muscle tissues, stomach and skeletal muscle, using a constant-rate infusion of the drug into rats. Further, to elucidate the distribution mechanism of acotiamide to the stomach, *in vitro* binding studies were performed with plasma and stomach tissue homogenate. The initial uptake clearance was also determined by integration plot analysis for several tissues, including stomach and skeletal muscle. Furthermore, to determine whether the distribution of acotiamide was concentrative, the stomach-to-plasma unbound concentration ratio ($C_{st,u,cyt}/C_{p,u}$) was determined.

4.2. Materials and methods

4.2.1. Chemicals

N-[2-[bis(1-methylethyl)amino]ethyl]-2-[(2-hydroxy-4,5-dimethoxybenzoyl)amino]thiazole-4-carboxamide monohydrochloride trihydrate (acotiamide hydrochloride, Z-338/YM443) and

(N-[2-(diisopropylamino)ethyl]-2-[(2,4,5-trimethoxybenzoyl)amino]-1,3-thiazole-4-carboxamide (ID951551, an internal standard for liquid chromatography) were synthesized in the central research laboratories of Zeria Pharmaceutical Co., Ltd. (Saitama, Japan).

[¹⁴C]Acotiamide (2.26 GBq/mmol) was synthesized by GE Healthcare UK Ltd.

(Buckinghamshire, England). [³H]Inulin (5.37 MBq/mg) was purchased from American Radiolabeled Chemicals, Inc. (St. Louis, MO). All other chemicals were reagent grade.

4.2.2. Animals

Male Sprague-Dawley rats (six to seven weeks of age) were obtained from Charles River Japan, Inc. (Kanagawa, Japan). Animals were housed under standard controlled environmental conditions at $23 \pm 3^{\circ}\text{C}$ and $55\% \pm 20\%$ humidity, with 12-hour light/dark cycles (7:00-19:00, light) and food (CRF-1; Oriental Yeast Co., Ltd., Tokyo, Japan) and water available *ad libitum*. The rats were allowed to acclimate to laboratory conditions for at least one week prior to performing the experiments. All animal experiments were approved by the Animal Care and Use Committee of the Central Research Laboratories of Zeria Pharmaceutical Co., Ltd.

4.2.3. *In vivo* infusion study

For the infusion of acotiamide, rats were first anesthetized with pentobarbital (50 mg/kg), and the femoral artery and vein were cannulated with heparinized polyethylene tubing. Acotiamide was dissolved in a 5% injectable glucose solution and then infused through the femoral vein cannula at a flow rate of 20 $\mu\text{l}/\text{min}$. The infusion rates were set at 2, 5, 10, 20, 50, and 100 nmol/min/kg. Serial blood samples were collected from the arterial cannula before and 60, 90, 100, 110, and 120 min after drug administration, and were then centrifuged to separate the plasma. The abdomen was opened 120 min after starting the infusion, and the stomach and skeletal muscle tissues were immediately excised, rinsed with distilled water, weighed, and homogenized in distilled water to form a 20% (w/v) homogenate. The concentrations of acotiamide in plasma, stomach tissue, and skeletal muscle tissue were determined by liquid chromatography mass spectrometry (LC-MS/MS), as described below.

4.2.4. Kinetic analysis of the *in vivo* stomach distribution of acotiamide

Total body clearance (CL_{tot}), which was based on *in vivo* infusion data, was calculated according to the following equation.

$$CL_{tot} = I_{rate}/C_{a,ss} \dots\dots\dots \text{Eq. 1-1}$$

where I_{rate} is the infusion rate of acotiamide, and $C_{a,ss}$ is the arterial plasma concentration of acotiamide 120 min after starting the infusion.

Kinetic parameters for the distribution of acotiamide were determined from the plasma and stomach tissue concentration data obtained from the acotiamide infusion using WinNonlin (Pharsight Corp., Mountain View, CA). The $K_{p,app,in vivo}$ of acotiamide was defined by the following equation:

$$K_{p,app,in vivo} = C_t/C_{a,ss} = \frac{C_{b,t} + C_{f,t}}{C_{f,p}/f_{u,p}} \dots\dots\dots \text{Eq. 1-2}$$

where C_t is the concentration of acotiamide in stomach tissue, $C_{b,t}$ and $C_{f,t}$ are the bound and unbound stomach tissue concentration of acotiamide, respectively, and $f_{u,p}$ is the unbound fraction of acotiamide in plasma (0.128), which was calculated from the plasma protein binding parameters under linear conditions, as described below, since the examined unbound plasma concentration was markedly lower than the dissociation constant *in vitro* ($K_{d,in vitro}$).

Assuming that both saturable and non-saturable binding are involved in tissue distribution, $C_{b,t}$ was defined by the following equation:

$$C_{b,t} = \frac{B_{max,in vivo} \cdot C_{f,t}}{(K_{d,in vivo} + C_{f,t})} + N_{in vivo} \cdot C_{f,t} \dots\dots\dots \text{Eq. 1-3}$$

Then, Eq. 1-2 can be expressed by:

$$K_{p,app,in vivo} = \frac{\left(\frac{B_{max,in vivo} \cdot C_{f,t}}{K_{d,in vivo} + C_{f,t}} + N_{in vivo} \cdot C_{f,t} \right) + C_{f,t}}{C_{f,p}/f_{u,p}} \dots\dots\dots \text{Eq. 1-4}$$

Assuming that the unbound concentration in stomach tissue ($C_{f,t}$) is equal to that of plasma ($C_{f,p}$) in Eq. 1-4:

$$K_{p,app,in vivo} = \frac{B_{max,in vivo}}{\left(\frac{K_{d,in vivo}}{f_{u,p}} + C_{a,ss}\right)} + (N_{in vivo} + 1) \cdot f_{u,p} \dots\dots\dots \text{Eq. 1-5}$$

where $B_{max,in vivo}$ is the binding capacity, $K_{d,in vivo}$ is the dissociation constant, and $N_{in vivo}$ is the proportionality constant for nonspecific binding, $C_{a,ss}$ represents the steady-state plasma concentration of acotiamide. The first and second terms on the right side of Eq. 1-5 describe the displaceable (saturable) K_p value ($K_{p,disp}$) and non-displaceable (non-saturable) K_p value ($K_{p,nondisp}$), respectively. The $K_{d,in vivo}$, $B_{max,in vivo}$, and $N_{in vivo}$ values were obtained by fitting the data sets of $K_{p,app,in vivo}$ and $C_{a,ss}$ to Eq. 1-5.

4.2.5. *In vitro* binding study

Rats were anesthetized, and plasma and stomach tissue were collected. The excised stomach tissue was rinsed with 250 mM sucrose containing 50 mM Tris-HCl buffer (pH 7.4), weighed, and homogenized in the identical buffer to form a 20% (w/v) homogenate.

The *in vitro* binding rates of acotiamide were determined by an ultracentrifugation method. Briefly, acotiamide was added to the 20% (w/v) homogenate of stomach tissue and the collected plasma to final concentrations of 0.05 to 10,000 μM and 0.01 to 2,000 μM , respectively, and the resulting mixtures were then ultracentrifuged at $220,000 \times g$ for 18 h at 4°C . The concentration of acotiamide in the supernatant following ultracentrifugation was determined by LC-MS/MS, as described below.

The unbound fraction ($f_{u,p}$ and $f_{u,homo}$ for plasma and stomach tissue homogenate, respectively) was calculated as follows:

$$f_{u,p} \text{ or } f_{u,homo} = C_{sup} / C_{sample} \dots\dots\dots \text{Eq. 1-6}$$

where C_{sample} is the nominal concentration in the stomach tissue or plasma sample, and C_{sup} is the concentration in the supernatant after ultracentrifugation.

The value of the unbound fraction in 100% of the stomach tissue homogenate ($f_{u,\text{homo}}$) was extrapolated from the observed f_u values ($f_{u,\text{homo}(20\%)}$) as follows [28]:

$$f_{u,\text{homo}} = \frac{1/d}{(1/f_{u,\text{homo}(20\%)} - 1) + 1/d} \dots\dots\dots \text{Eq. 1-7}$$

where d is the dilution factor (equal to 5) for the stomach tissue homogenate.

4.2.6. Determination of binding parameters

Parameters for binding to plasma and stomach tissue were calculated using Eq. 1-8 and Eq. 1-9, respectively.

$$C_b = \frac{B_{\text{max},\text{in vitro}} \cdot C_f}{K_{d,\text{in vitro}} + C_f} + N_{\text{in vitro}} \cdot C_f \dots\dots\dots \text{Eq. 1-8}$$

$$C_b = N_{\text{in vitro}} \cdot C_f \dots\dots\dots \text{Eq. 1-9}$$

where C_b and C_f are the bound and unbound, respectively, stomach tissue or plasma concentrations of acotiamide, $B_{\text{max},\text{in vitro}}$ is the binding capacity, $K_{d,\text{in vitro}}$ is the dissociation constant, and $N_{\text{in vitro}}$ is the proportionality constant for nonspecific binding. The above equation was fit to the binding data sets to obtain estimates of binding parameters by the nonlinear least squares method using WinNonlin.

The unbound fraction of acotiamide in plasma ($f_{u,p}$) and stomach tissue ($f_{u,t}$) in the linear region was estimated from the binding parameters by Eq. 1-10 and Eq. 1-11, respectively.

$$f_{u,p} = \frac{1}{1 + \frac{B_{\text{max},\text{in vitro}}}{K_{d,\text{in vitro}}} + N_{\text{in vitro}}} \dots\dots\dots \text{Eq. 1-10}$$

$$f_{u,t} = \frac{1}{1 + N_{\text{in vitro}}} \dots\dots\dots \text{Eq. 1-11}$$

The *in vitro* tissue-to-plasma concentration ratio ($K_{p,app,in vitro}$) was predicted from the *in vitro* tissue binding data alone, without assuming the existence of any concentrative influx and/or efflux processes, and was expressed as follows:

$$K_{p, app, in vitro} = f_{u,p} / f_{u,t} \dots\dots\dots \text{Eq. 1-12}$$

4.2.7. Integration plot analysis

Rats were anesthetized with pentobarbital (50 mg/kg), and the femoral artery was cannulated with heparinized polyethylene tubing. After intravenous bolus administration of [¹⁴C]acotiamide (0.185, 0.924, 1.85, and 9.24 μmol/kg) including [³H]inulin (0.1 mg/kg), blood samples were collected from the arterial cannula at 10, 20, 30, and 45 s, and at 1, 1.5, 2, 3, and 5 min. In addition, at the 30 s, and 1, 2, 3, and 5 min time points, the abdomen was opened, and the stomach, skeletal muscle, liver, kidney, and brain tissues were excised and the tissue weights were then measured. After solubilization of the tissue samples with a Soluen-350 tissue solubilizer (PerkinElmer, Waltham, MA), the radioactivities in blood and tissues were measured using a TRI-CARB 2900TR liquid scintillation analyzer (PerkinElmer).

When tissue uptake of acotiamide was measured within a short time period, during which the efflux and/or elimination of radioactivity from tissues were negligible, tissue distribution was described by linear kinetics, as described by Eq. 1-13.

$$dX_t / dt = CL_{inf,app} \cdot C_{b,t} \dots\dots\dots \text{Eq. 1-13}$$

where X_t is the amount of [¹⁴C]acotiamide in the tissue at time t , $CL_{inf,app}$ is the initial uptake clearance, and $C_{b,t}$ is the blood concentration of acotiamide at time t . Integration of Eq. 1-13 gives

$$X_t = CL_{inf,app} \cdot AUC_{0-t} + V_d \cdot C_{b,t} \dots\dots\dots \text{Eq. 1-14}$$

where AUC_{0-t} represents the area under the C_b time curve from time 0 to t, V_d represents the distribution volume of tissue compartments that equilibrates rapidly with the blood compartment. Eq. 1-14 divided by $C_{b,t}$ gives

$$K_p = X_t / C_{b,t} = CL_{inf,app} \cdot AUC_{0-t} / C_{b,t} + V_d \dots\dots\dots \text{Eq. 1-15}$$

where K_p ($X_t/C_{b,t}$) is the tissue-to-blood concentration ratio at time t, with units of milliliters per gram of tissue.

The $CL_{inf,app}$ was obtained from the slope of the plot of $X_t/C_{b,t}$ (on the ordinate) vs. $AUC_{0-t}/C_{b,t}$ (on the abscissa) [29, 30]. The initial uptake clearance ($CL_{inf,r}$) for the kidney was determined from $CL_{inf,app}$, $f_{u,b}$, and glomerular filtration rate (GFR) by use of the following equation:

$$CL_{inf,r} = CL_{inf,app} - f_{u,b} \cdot GFR \dots\dots\dots \text{Eq. 1-16}$$

where the GFR was taken as the $CL_{inf,app}$ of inulin, $f_{u,b}$ is the unbound fraction of acotiamide in the blood, which was calculated by dividing $f_{u,p}$ by the blood-to-plasma concentration ratio (0.84), and $CL_{inf,app}$ represents a hybrid parameter of the permeability-surface area product ($PS_{inf,app}$) and blood flow (Q, ml/min/g of tissue). The blood-flow independent parameter, $f_{u,b} \cdot PS_{inf,app}$ was calculated using Eq. 1-17 assuming the well-stirred model [31, 32].

$$f_{u,b} \cdot PS_{inf,app} = \frac{CL_{inf,app} \cdot Q}{Q - CL_{inf,app}} \dots\dots\dots \text{Eq. 1-17}$$

where Q was calculated from tissue weight and tissue blood flow. The tissue weight and blood flow parameters for each tissue were taken from Hosseini-Yeganeh and McLachlan [33]. Tissue weight was converted from the tissue volume based on the assumption that tissue specific gravity equals 1 g/ml.

4.2.8. Determination of the stomach-to-plasma unbound concentration ratio of acotiamide

Plasma and stomach tissue homogenate were prepared from rats infused with 2 nmol/min/kg acotiamide in the identical manner as described for the *in vivo* infusion experiment, with the exception of the homogenate solvent used. Stomach tissue was homogenized in 250 mM sucrose containing 50 mM Tris-HCl buffer (pH 7.4) to form a 20% (w/v) homogenate. A portion of stomach tissue homogenate was centrifuged at $105,000 \times g$ for 60 min at 4°C to obtain the cytosol fraction. The remaining stomach tissue homogenate, cytosol fraction, and plasma were ultracentrifuged at $220,000 \times g$ for 18 h at 4°C, and the resultant supernatants were collected. The concentrations of acotiamide in the plasma, stomach tissue homogenate, cytosol, and collected supernatants were determined by LC-MS/MS, as described below.

The unbound fraction (f_u) of acotiamide was calculated as described for the *in vitro* binding study. The fraction of acotiamide distributed to the cytosol was calculated as follows:

$$Fract_{cyt} = \frac{(1 + d(1/f_{u,cyt(20\%)} - 1))}{(1 + d(1/f_{u,homo(20\%)} - 1))} \dots\dots\dots Eq. 1-18$$

where d is the dilution factor (equal to 5) for the stomach tissue homogenate, and $f_{u,cyt(20\%)}$ and $f_{u,homo(20\%)}$ are the unbound fractions in the cytosol and stomach tissue homogenate, respectively. The unbound concentration of acotiamide in the cytosol fraction ($C_{st,u,cyt}$) was calculated as follows:

$$C_{st,u,cyt} = C_{st} \cdot Fract_{cyt} \cdot f_{u,cyt} \dots\dots\dots Eq. 1-19$$

where C_{st} represents the concentration of acotiamide in the stomach tissue, and $f_{u,cyt}$ is the unbound fraction in 100% of the cytosol fraction extrapolated from the observed f_u values ($f_{u,cyt(20\%)}$). The $C_{st,u,cyt}$ was adjusted based on the assumption that the specific

gravity of the cytosolic fluid volume is equal to 1 g/ml of tissue. The unbound concentration ratio of stomach cytosol to plasma ($C_{st,u,cyt}/C_{p,u}$) was then calculated.

4.2.9. Quantification of acotiamide by LC-MS/MS

For the quantification of acotiamide, 50 μ l of each plasma sample was mixed with 10 μ l 50% methanol, and 500 μ l methanol and an internal standard were then added to the resulting solutions. After centrifuging the mixtures, the supernatants were collected and subjected to LC-MS/MS.

For the stomach and skeletal muscle tissues, 100 μ l of each homogenate was mixed with 20 μ l 50% methanol, and 480 μ l methanol was then added to the resulting solutions. Following centrifugation, an internal standard was added to 400 μ l of supernatant, and 300 μ l of this mixture was filtrated using a centrifugal filter. Following filtration, 75 μ l distilled water was added to the filtrate, and 10 μ l aliquots were then subjected to LC-MS/MS.

Acotiamide in the cytosol fraction and the supernatants of plasma, stomach tissue homogenate, and cytosol fraction was quantitated by first mixing 200 μ l of each sample with 20 μ l dimethylsulfoxide, and 200 μ l 5% phosphoric acid and an internal standard were then added to the resulting solutions. The mixtures were applied to an Oasis HLB μ Elution solid-phase extraction plate (Waters, Milford, MA), and the analytes were eluted with 100 μ l methanol. Distilled water (100 μ l) was added to each eluate, and 10 μ l aliquots were then subjected to LC-MS/MS.

LC-MS/MS analysis was performed on an API 4000 tandem mass spectrometer (Applied Biosystems, Inc., Foster City, CA) equipped with a 1100 series HPLC system (Agilent Technologies, Palo Alto, CA) using a reverse phase column (CAPCELL PAK C_{18} MGII; Shiseido, Tokyo, Japan). Electrospray ionization was performed in the positive-ion

mode. Acotiamide and an internal standard were quantified using the selected reaction-monitoring mode with a flow rate of 0.8 ml/min methanol/20 mM ammonium acetate (pH 6.0) (6: 4). The monitoring ions for acotiamide and the internal standard were m/z 451 \rightarrow m/z 271 and m/z 465 \rightarrow m/z 364, respectively.

4.3. Results

4.3.1. Distribution of acotiamide to the stomach and skeletal muscle in rats

The distribution of acotiamide to the stomach and skeletal muscle of rats was determined after constant-rate infusion of several doses of acotiamide for 120 min (Fig. 2-1). At each infusion dose, the plasma concentrations of acotiamide maintained a steady level for 30 min until the termination of infusion (data not shown). The tissue-to-plasma concentration ratio ($K_{p,app,in vivo}$) of acotiamide for the stomach was 4.1 ± 0.3 and 2.4 ± 0.3 ml/g of tissue at 2 nmol/min/kg and 100 nmol/min/kg, respectively, indicating that the stomach distribution was dependent on the plasma concentration (Fig. 2-1). In contrast, the $K_{p,app,in vivo}$ for skeletal muscle was independent of the plasma acotiamide concentration, with values of approximately 0.8 ml/g of tissue determined for all infusion doses (Fig. 2-1). The total body clearances (CL_{tot}) of acotiamide ranged from 34.1 ± 6.1 to 38.7 ± 3.9 ml/min/kg at all examined doses, and increasing the infusion rate did not affect the CL_{tot} .

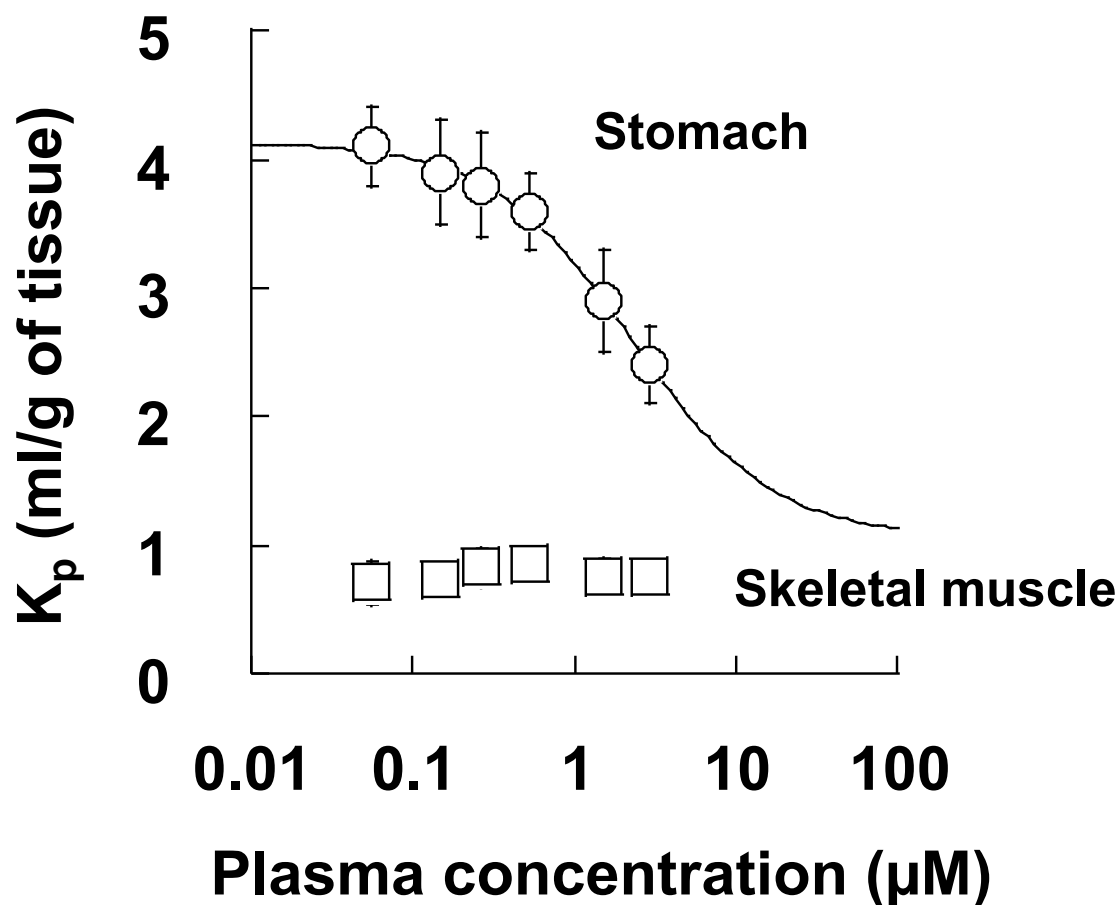


Fig. 2-1. Tissue-to-plasma concentration ratio (K_p) versus plasma concentration in rat stomach and skeletal muscle 120 min after starting constant-rate infusion of acotiamide.

Acotiamide was infused at rates of 2, 5, 10, 20, 50, and 100 nmol/min/kg. The solid line represents the calculated curve obtained by fitting to Eq. 1-5 (see the Materials and methods). $K_{d,in vivo} = 0.292$ (0.062) μM , $B_{max,in vivo} = 7.00$ (2.08) nmol/g of tissue, and $N_{in vivo} = 7.30$ (2.32); the values in parentheses represent the S.E. for the nonlinear least squares analysis. The data points and error bars represent the mean \pm S.D. of six independent experiments.

4.3.2. Binding parameters for acotiamide calculated from *in vivo* infusion study.

The *in vivo* binding parameters of acotiamide were calculated according to Eq. 1-5 using the data obtained from the *in vivo* constant-rate infusion experiments (Fig. 2-1). The dissociation constant for the saturable component ($K_{d,in vivo}$) was determined to be 0.292 μM .

4.3.3. Plasma and stomach tissue protein binding of acotiamide

To evaluate the involvement of tissue protein binding in acotiamide distribution, the binding of acotiamide to plasma and stomach tissue protein was next examined (Fig. 2-2). The binding of acotiamide to plasma protein was concentration dependent (Fig. 2-2A), indicating two components involved. In contrast, the binding of acotiamide by stomach tissue protein showed a linear relationship with the concentration of acotiamide (Fig. 2-2B). The binding parameters for the two processes are summarized in Table 2-1. In addition, we also predicted the $K_{p,app,in vitro}$ from the unbound fraction of acotiamide in the plasma and stomach tissue, which was determined to be 2.2 (Table 2-1).

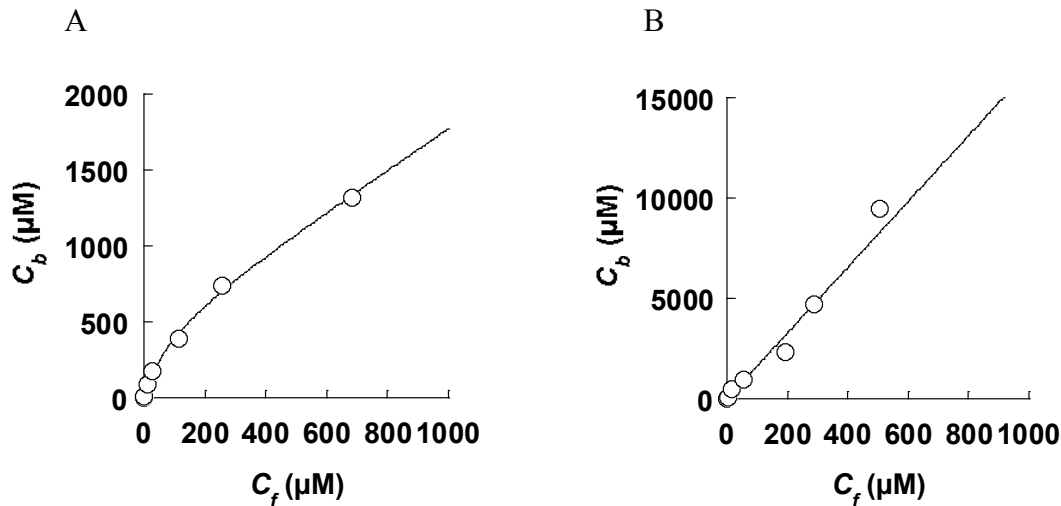


Fig. 2-2. Protein binding of acotiamide by plasma (A) and stomach tissue (B).

Each data point represents the mean value of triplicate samples. C_b represents the concentration of acotiamide bound to plasma or stomach tissue protein, and C_f is the unbound concentration of acotiamide. C_b and C_f of the stomach were expressed as 100% of the stomach tissue. The solid line in A and B represents the fitted line (corresponding to Eq. 1-8 and 1-9, respectively).

Table 2-1. The binding parameters of acotiamide, free fractions in plasma and stomach tissue, and stomach tissue-to-plasma concentration ratio

| Matrices | $B_{max,in vitro}^a$ | $K_{d,in vitro}$ (μM) | $N_{in vitro}$ | f_u | $K_{p,app,in vitro}$ |
|----------|----------------------|---------------------------------------|----------------|--------|----------------------|
| Plasma | 479 (102) | 87.0 (25.2) | 1.33 (0.14) | 0.128 | 2.2 |
| Stomach | — | — | 16.4 (1.0) | 0.0575 | |

^a The unit is μM and nmol/g of tissue for plasma and stomach, respectively. The values in parentheses represent the S.E. for the nonlinear least squares analysis.

4.3.4. Integration plot analysis

The time profiles of acotiamide concentrations in the blood and various tissues were subjected to kinetic analyses after intravenous bolus administration of acotiamide at multiple doses. The unbound blood concentration ranged from 0.116 to 7.42 μM at the initial sampling point of the tissues (30 s) for doses ranging from 0.185 to 9.24 $\mu\text{mol/kg}$, suggesting that the uptake experiments were conducted in the concentration range including $K_{d, \text{in vivo}}$. In Fig. 2-3, the $X_t/C_{b,t}$ and $\text{AUC}_{0-t}/C_{b,t}$ are plotted (integration plot) at an acotiamide dose of 0.185 $\mu\text{mol/kg}$, with the slope of each curve corresponding to the initial tissue uptake clearance ($CL_{\text{inf,app}}$). Notably, the slope for acotiamide was markedly larger than that for inulin, an extracellular marker, in the stomach and liver (Fig. 2-3A and Fig. 2-3D, respectively), and was slightly larger than that for inulin in the skeletal muscle and kidney (Fig. 2-3B and Fig. 2-3E, respectively). In brain tissue, however, the slope for acotiamide was almost equal to that for inulin (Fig. 2-3C). The $CL_{\text{inf,app}}$ for acotiamide in the stomach, liver, and kidney was higher than that in the skeletal muscle and brain. In all of the examined tissues, $f_{u,b} \cdot PS_{\text{inf,app}}$, which is independent of blood flow, was calculated using the $CL_{\text{inf,app}}$ in the well-stirred model and was found to decrease with increasing acotiamide dosage for all examined tissues, with the exception of the brain (Fig. 2-4). The $f_{u,b} \cdot PS_{\text{inf,app}}$ was lower than the blood flow rate in the stomach, skeletal muscle, and brain at the lowest dose of acotiamide (Fig. 2-4).

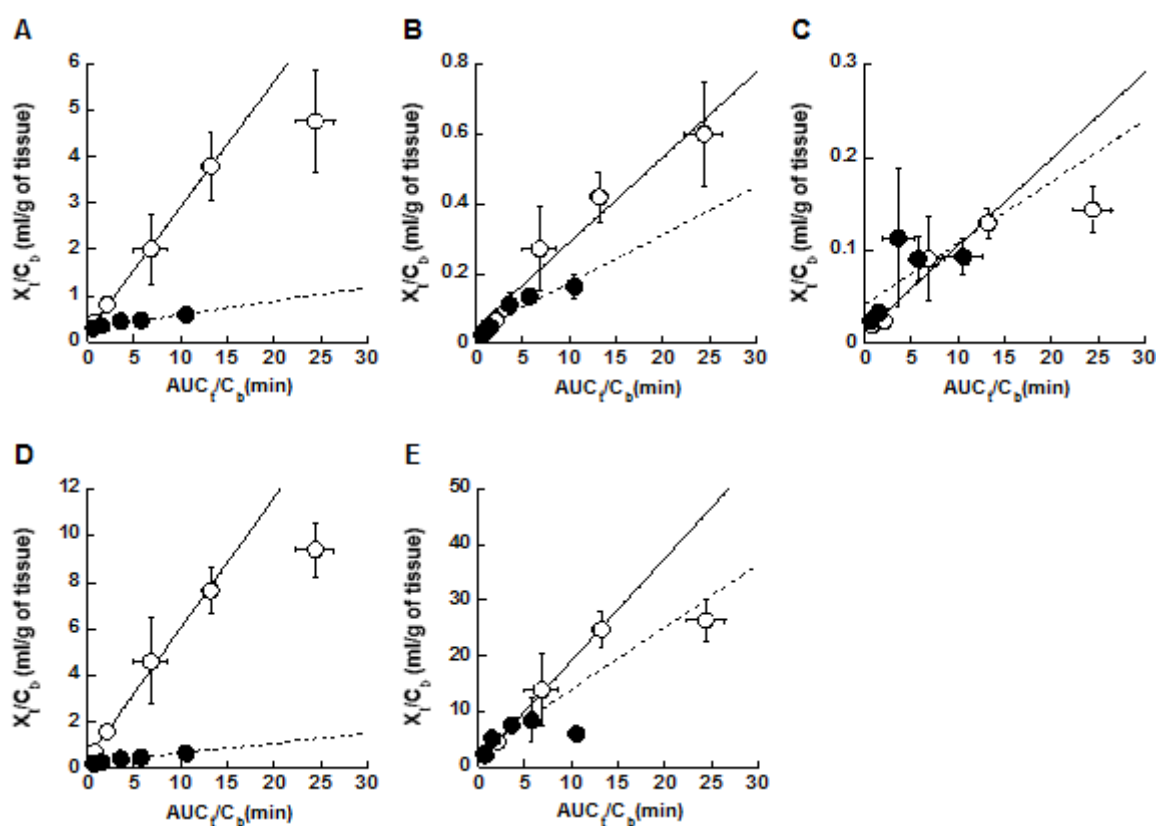


Fig. 2-3. Integration plots representing acotiamide uptake by each examined tissue.

Time profiles of acotiamide concentration in the blood and stomach (A), skeletal muscle (B), brain (C), liver (D), and kidney (E) were determined after bolus injection (0.185 $\mu\text{mol/kg}$) into rats. The slope represents the initial uptake clearance of acotiamide, which was determined to be 0.269, 0.0242, 0.00922, 0.558, and 1.49 ml/min/g of tissue for the stomach, skeletal muscle, brain, liver, and kidney, respectively. The broken line in the integration plots represents the uptake of [³H]inulin. The data points and error bars represent the mean \pm S.D. of three independent experiments.

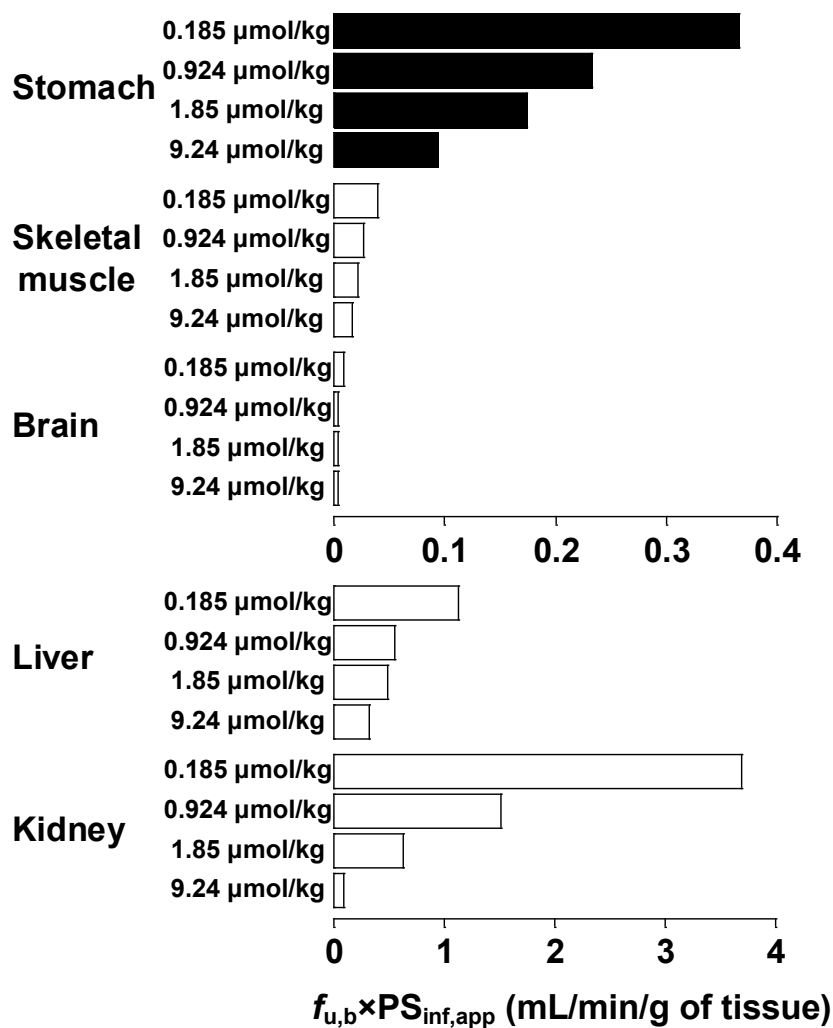


Fig. 2-4. $f_{u,b} \cdot PS_{inf,app}$ for acotiamide in various tissues after intravenous bolus administration. Tissue blood flow was 1.0, 0.061, 1.1, 1.1, and 2.5 ml/min/g of tissue for the stomach, skeletal muscle, brain, liver, and kidney, respectively, in rat (body weight 250 g) [33].

4.3.5. Unbound concentration ratio of stomach to plasma

To determine whether the distribution of acotiamide was concentrative, the stomach-to-plasma unbound concentration ratio ($C_{st,u,cyt}/C_{p,u}$) was determined. The free fractions of acotiamide in the examined biological matrices are summarized in Table 2. The fraction of acotiamide distributed to the stomach cytosol ($Fract_{cyt}$) is also listed in Table 2. From these calculations, the $C_{st,u,cyt}/C_{p,u}$ was determined to be 2.8 ± 0.8 (Table 2).

Table 2-2. The unbound concentration ratio of stomach to plasma ($C_{st,u,cyt}/C_{p,u}$) after the constant-rate infusion of acotiamide at a dose of 2 nmol/min/kg to rats

| Matrices | f_u | Fract _{cyt} ^a | Concentration (μ M) | $C_{st,u,cyt}/C_{p,u}$ |
|----------|---------------------|-----------------------------------|--------------------------|------------------------|
| Plasma | 0.149 ± 0.041 | – | 0.00739 ± 0.00319^b | – |
| Stomach | 0.868 ± 0.126^c | 0.120 ± 0.033 | 0.0193 ± 0.0063^d | 2.8 ± 0.8 |

^a Fraction of acotiamide distributed to the stomach cytosol.

^b Unbound concentration of acotiamide in plasma ($C_{p,u}$, μ M).

^c Unbound fraction extrapolated from $f_{u,cyt(20\%)} (f_{u,cyt})$.

^d Unbound concentration of acotiamide in the stomach cytosol ($C_{st,u,cyt}$).

Each value represents the mean \pm S.D. of six rats.

4.4. Discussion

Acotiamide hydrochloride (Z-338/YM443) is a member of new class of gastroprokinetic agents currently being developed for the treatment of FD. It is thought that acotiamide ameliorates symptoms of FD by improving delayed gastric emptying through inhibition of AChE in the stomach. However, as AChE distributes to various tissues, including muscle and brain, the objective of the present study was to assess the distribution of acotiamide to tissues, and to elucidate the mechanism for the distribution of acotiamide to the stomach.

The distribution of drugs in the body is determined by numerous factors, including tissue blood flow, basolateral membrane permeability, and cell-binding components. The mechanisms for the selective tissue distribution of drugs are likely to involve tissue binding, higher tissue uptake, and/or lower efflux from tissues. Here, to determine the total sum of these mechanisms, the distribution of acotiamide was initially evaluated at steady state. The tissue-to-plasma concentration ratio ($K_{p,app,in vivo}$) of stomach tissue was higher than unity at all examined doses (Fig. 2-1). The $K_{p,app,in vivo}$ of stomach tissue decreased with increasing plasma concentrations of acotiamide ($C_{a,ss}$), indicating that a saturable component was involved in the stomach distribution (Fig. 2-1). Therefore, we speculate that the distribution of acotiamide into the stomach involves a specific mechanism.

The contribution of tissue protein binding on the distribution of drugs has previously been reported by Wierzba et al. [34], who demonstrated that the tissue distribution of vincristine could be predicted by tubulin concentrations in the respective tissues [34]. Here, the binding parameters of acotiamide were estimated from *in vivo* infusion experiments. The *in vivo* dissociation constant ($K_{d,in vivo}$) was estimated to be 0.292 μM (Fig. 2-1), indicating that a component specifically interacts with acotiamide in the stomach. However, *in vitro* binding revealed that stomach protein binding did not saturate at acotiamide concentrations between 0.05 to 10,000 μM (Fig. 2-2B), although the $K_{p,app,in vivo}$ decreased by approximately 60% of the highest value for the unbound plasma concentration of acotiamide (0.380 μM) at the highest infusion rate (Fig. 2-1). The $K_{p,app,in vitro}$, which was predicted to be 2.2 from free fractions of the plasma and stomach tissue based on Eq. 1-12, was not consistent with the $K_{p,app,in vivo}$ at a dose of 2 nmol/min/kg (Table 2-1, Fig. 2-1). However, at a dose of 100 nmol/min/kg, the $K_{p,app,in vivo}$ was determined to be 2.4 ml/g of tissue, which was consistent with $K_{p,app,in vitro}$, suggesting that the nonspecific binding of acotiamide to stomach tissue proteins may be involved in the distribution of acotiamide into stomach tissue at the highest examined infusion rate (Table 2-1, Fig. 2-1). Since $K_{p,app,in vivo}$ was larger than $K_{p,app,in vitro}$ at the lowest infusion rate of acotiamide, a mechanism other than tissue protein binding appears to be involved in the specific distribution of acotiamide into the stomach.

Transporters are actively involved in the specific distribution of drugs to target organs. The transporter responsible for the uptake of xenobiotics across basolateral membranes has been identified in clearance organs, including the liver and kidney [35,36,37]. However, no transport proteins that are able to facilitate the uptake of a wide variety of xenobiotics from intra-vascular spaces to the stomach have been identified. To evaluate the involvement of transport in the distribution of acotiamide, the initial uptake clearance

($CL_{inf,app}$) was determined. The saturable uptake of acotiamide by stomach tissue was observed at the blood unbound concentration range from 0.116 to 7.42 μM (Fig. 2-3A), while the $K_{p,app,in vivo}$ also showed saturation at the unbound concentration range of 0.00699 to 0.380 μM (Fig. 2-1). As these concentration ranges are similar, uptake processes appear to play a role in the specific distribution of acotiamide to the stomach. In addition, the $f_{u,b} \cdot PS_{inf,app}$ was lower than the blood flow rate in stomach tissue, suggesting that the permeability of acotiamide might be the rate-limiting step in the uptake by stomach tissue (Fig. 2-4). Moreover, the unbound concentration ratio of stomach to plasma ($C_{st,u,cyt}/C_{p,u}$), which is minimally affected by the tissue binding to cytosolic proteins or organelles, was higher than unity (Table 2-2). These findings suggest that an active transport system is involved in the distribution of acotiamide to the stomach.

We determined that the $K_{p,app,in vivo}$ of skeletal muscle (approximately 0.8 ml/g of tissue) was independent of the $C_{a,ss}$ (Fig. 2-1), while the $f_{u,b} \cdot PS_{inf,app}$ exhibited only minimal dose dependence (Fig. 2-4). This discrepancy likely resulted from the experimental conditions, as the uptake study was performed within a short time period to facilitate monitoring of only the uptake process, during which time the efflux and/or elimination from the tissues were negligible, whereas the conditions of the constant-rate infusion experiments may have been closer to physiological conditions. Thus, the transport of acotiamide may only minimally contribute to the distribution to skeletal muscle. Taken together, these results indicate that carrier-mediated concentrative uptake processes (i.e., transport systems) play an important role in the distribution of acotiamide to the stomach, but not the skeletal muscle, in rats.

In contrast to a number of other motility modifying drugs, acotiamide does not increase prolactin levels or extrapyramidal symptoms during or after the period of exposure [38]. Here, we clearly demonstrated that acotiamide does not distribute to the brain, because the

X_t/C_b for acotiamide was less than or equal to the X_t/C_b for inulin in the examined brain tissues (Fig. 2-3). Since the $f_{u,b} \cdot PS_{inf,app}$ of the brain was approximately 100-fold lower than the blood flow rate (Fig. 2-4), it appears the blood-brain barrier prevents acotiamide from penetrating the brain. The poor distribution of acotiamide to the brain is a desirable pharmacological property of this novel AChE inhibitor.

Following oral administration, acotiamide is mainly metabolized to glucuronide conjugates through reactions catalyzed by members of the human uridine 5'-diphosphate-glucuronosyltransferase (UGT) 1A family, particularly UGT1A9 and 1A8 [39]. Messenger RNAs of UGTs have also been detected in the kidney and liver in rats [40,41]. In the present study, the $f_{u,b} \cdot PS_{inf,app}$ of the rat kidney and liver was equal to or higher than the blood flow rate of each tissue at a dose of 0.185 $\mu\text{mol/kg}$ (Fig. 2-4). In addition, the sum of the $CL_{inf,app}$ of the kidney and liver at a dose of 0.185 $\mu\text{mol/kg}$, which was extrapolated to whole tissues based on the weight of each tissue of whole animals (22.1 and 23.0 ml/min/kg, respectively), was close to the total body clearance based on the blood concentration (40.6 to 46.1 ml/min/kg), which was converted from the CL_{tot} values obtained from the constant-rate infusion study. Taken together, these findings suggest that the overall elimination of acotiamide is governed by tissue uptake processes in the liver and/or kidney of rats.

In conclusion, we have demonstrated that acotiamide is selectively distributed to the stomach in rats, and that the specific distribution may be mediated by a carrier-mediated uptake process. Thus, acotiamide appears to be a promising and highly selective drug for the treatment of FD.

4.5. Summary

Acotiamide improves gastric motility by inhibiting AChE activity in stomach; however, the mechanism of distribution of acotiamide from blood to stomach has not been clarified. Here, the tissue distribution of acotiamide was investigated in rats. The tissue-to-plasma concentration ratio ($K_{p,app,in vivo}$) for stomach decreased from 4.1 to 2.4 ml/g of tissue at steady state with increasing plasma concentrations, whereas the $K_{p,app,in vivo}$ for skeletal muscle was much lower and constant regardless of the concentration of acotiamide in plasma. *In vitro* binding to stomach tissue protein exhibited a linear profile, with a predicted $K_{p,app,in vitro}$ of 2.2 from free fractions under linear conditions. Therefore, protein binding to stomach tissue might only play a limited role in the stomach distribution of acotiamide. The influx permeability ($f_{u,b} \cdot PS_{inf,app}$) in the stomach exhibited dose-dependent saturation at the lowest range of examined blood unbound concentrations of acotiamide, whereas that in skeletal muscle exhibited only minimal dose dependence. In addition, the unbound concentration ratio of stomach to plasma (2.8) at steady state was markedly higher than unity. Taken together, these results suggest that carrier-mediated concentrative uptake processes play an important role in the distribution of acotiamide to the stomach, but not skeletal muscle.

5. Physiologically-based pharmacokinetic and pharmacodynamic modeling for the inhibition of acetylcholinesterase by acotiamide, a novel gastroprokinetic agent for the treatment of functional dyspepsia, in rat stomach

5.1. Introduction

In previous chapter, acotiamide was highly distributed into the stomach after the intravenous administration of acotiamide to rats [20]. Moreover, the integration plot analysis indicated that acotiamide was uptaken by at least two stomach compartments, which rapidly and slowly equilibrated with the blood [20]. However, as the role of these stomach compartments were unsettled, the relationship of the blood and stomach concentration of acotiamide with the pharmacological action remains unclear.

The purpose of this study was to elucidate the relationship of the blood and stomach concentration of acotiamide with the pharmacological action. For the purpose, we developed a physiologically-based pharmacokinetic and pharmacodynamic (PBPK/PD) model to describe the profiles for concentration of acotiamide and ACh in rats. In this model, the stomach compartments rapidly and slowly equilibrated with the blood were assumed as vascular space and extravascular compartment in rat stomach, respectively. In addition, ACh was chosen as the marker for the pharmacological action of acotiamide because the reported index like the motility index might be improper for the describing the time course change for the pharmacological action of acotiamide. The profiles for blood and stomach concentration of acotiamide were determined to characterize the pharmacokinetic parameters. Moreover, to confirm the elevation of ACh derived from the inhibition of AChE by acotiamide, the inhibitory effect of acotiamide on AChE *in vitro* and the increase of ACh in the stomach were determined.

5.2. Materials and Methods

5.2.1. Chemicals

N-[2-[bis(1-methylethyl)amino]ethyl]-2-[(2-hydroxy-4,5-dimethoxybenzoyl)amino]thiazole-4-carboxamide monohydrochloride trihydrate (acotiamide hydrochloride, Z-338/YM443 and N-[2-(diisopropylamino)ethyl]-2-[(2,4,5-trimethoxybenzoyl)amino]-1,3-thiazole-4-carboxamide (ID951551, an internal standard for the determination of acotiamide) were synthesized in the central research laboratories of Zeria Pharmaceutical Co., Ltd. (Saitama, Japan). 1,1-Dimethyl-4-acetylthiomethylpiperidinium iodide (MATP+) was purchased from Dojindo Laboratories (Kumamoto, Japan). 5,5'-Dithiobis-2-nitrobenzoic acid (DTNB), and (\pm)-sulpiride (an internal standard for the determination of MATP+-TNB) were purchased from Sigma-Aldrich Co. LLC (St Louis, MO, USA). Acetylcholine iodide and N-ethylmaleimide (NEM) were purchased from Wako Pure Chemical Industries (Osaka, Japan). Acetylcholine-d9 chloride (an internal standard for the determination of ACh) was purchased from Toronto Research Chemicals Inc. (Ontario, Canada). All other chemicals were reagent grade.

5.2.2. Animals

Male Sprague-Dawley rats (aged 6 to 7 weeks) obtained from Charles River Japan, Inc. (Kanagawa, Japan) were housed under standard controlled environmental conditions at $23 \pm 3^\circ\text{C}$ and $55\% \pm 20\%$ humidity, with a 12-h light/dark cycle (7:00-19:00, light) and food (CRF-1; Oriental Yeast Co., Ltd., Tokyo, Japan) and water available *ad libitum*. Rats were allowed to acclimate to laboratory conditions for at least one week prior to performing the experiments. All animal experiments were approved by the Animal Care and Use Committee of the Central Research Laboratories of Zeria Pharmaceutical Co., Ltd.

5.2.3. Preparation of stomach homogenate for *in vitro* study

Rats were anesthetized with isoflurane and their stomachs immediately excised after blood removal, rinsed with distilled water, weighed, and homogenized in distilled water to form a 50% (w/v) homogenate. Protein concentrations were determined using the Bio-Rad protein assay kit (Bio-Rad, Hercules, CA, USA).

5.2.4. AChE activity by stomach homogenate

AChE activity was measured using MATP⁺ as a substrate (50 μ M), as previously described [42]. Normally, MATP⁺ is hydrolyzed by AChE and reacted with DTNB. The release of TNB is generally measured with a spectrophotometer at 412 nm to determine AChE activity. However, in the present study, background absorbance was extremely high in stomach homogenate (50% [w/v]), which compromised the results. We therefore measured the concentration of the MATP⁺ and TNB complex (MATP⁺-TNB), which was the result of MATP⁺ hydrolysis by AChE, using ultra-performance liquid chromatography (UPLC; Waters, Milford, MA, USA).

The reaction medium (0.1 M Na₂HPO₄ and 0.1 M NaH₂PO₄ including 0.5% Triton[®] X-100, pH8.0) contained 10 mM DTNB and 2 mM NEM. Hydrolysis of MATP⁺ by AChE was initiated by adding 50 μ M MATP⁺ to an incubation medium that included the stomach homogenate after preincubation at 30°C for 3 min. At designated times, 1 ml of methanol containing 0.1% formic acid was added to terminate the reaction, and an internal standard ([\pm]-sulpiride) was then added. Following centrifugation, the supernatant was evaporated until dry under nitrogen gas in a water bath at 60°C and the residue was dissolved in 200 μ l of mobile phase B (see below for composition). The concentration of MATP⁺-TNB in each sample was determined by UPLC using a hydrophilic interaction chromatography (HILIC) column (ACQUITY[®] UPLC BEH HILIC; Waters) with MATP⁺

as the standard. Ultraviolet absorbance was monitored at 230 nm. Mobile phase A consisted of methanol and 5 mM ammonium acetate (pH5.0) (50:50). Mobile phase B consisted of acetonitrile, isopropanol and 5 mM ammonium acetate (pH5.0) (90:5:5). A steady gradient started at 1% mobile phase A for 5 min at a flow rate of 1.0 ml/min, moving then to 50% mobile phase B over the next 4 min, and finally to 1% mobile phase A from 9 to 12 min.

The initial hydrolysis velocity was calculated using linear regression of the data taken at 60 s. The effect of acotiamide on the MATP+ hydrolysis was studied at acotiamide concentrations ranging from 0.05 to 25 μ M.

5.2.5. *In vivo* study

For the intravenous administration of acotiamide, rats were first anesthetized with isoflurane. Acotiamide was dissolved in a 5% glucose solution and then injected to sixty-six rats in six different experiments via the femoral vein at 1.85 μ mol/kg. Blood samples were collected from the abdominal aorta at 5, 10, 15, and 30 min and 1, 2, 4, 6, 8, 24 and 48 h after drug administration and then centrifuged to separate the plasma. In addition, at each time point, the stomach was immediately excised, rinsed with distilled water, weighed, and homogenized in distilled water to form a 50% (w/v) homogenate. A portion of the homogenate from 5 min to 4 h was set aside for the determination of ACh, and the remainder was used for the determination of acotiamide concentration. The concentrations of acotiamide in plasma and stomach tissue and of ACh in stomach tissue were determined via liquid chromatography-mass spectrometry (LC-MS/MS) as described below.

5.2.6. Quantification of acotiamide by LC-MS/MS

For the quantification of acotiamide, 250 μ l of each plasma sample was mixed with 10 μ l of 50% methanol, 250 μ l of 2% trichloroacetate, and an internal standard. The mixtures were applied to an Oasis HLB μ Elution solid-phase extraction plate (Waters), and analytes were eluted with 100 μ l of methanol. Distilled water (100 μ l) was added to each elute, and 10- μ l aliquots were then subjected to LC-MS/MS.

For the stomach tissue, the stomach homogenate was further diluted with the same volume of distilled water to the homogenate. Thereafter, 10 μ l of 50% methanol and 200 μ l of 2% trichloroacetate were added to the solution. Following centrifugation, an internal standard was added to 300 μ l of supernatant. The solution was applied to an Oasis HLB μ Elution solid-phase extraction plate, and the analytes were eluted with 40 μ l methanol. Distilled water (40 μ l) was added to each elute, and 20- μ l aliquots were then subjected to LC-MS/MS.

LC-MS/MS analysis was performed on an API 4000 tandem mass spectrometer (ABSciex, Foster City, CA, USA) equipped with a solvent delivery system (LC-30AD) and auto-injector (SIL-30AC; both from Shimadzu, Kyoto, Japan) using a reverse phase column (CAPCELL PAK C₁₈ MGII; Shiseido, Tokyo, Japan). Electrospray ionization was performed in the positive-ion mode. Acotiamide and an internal standard were quantified using the selected reaction-monitoring mode with a flow rate of 0.8 ml/min methanol/20 mM ammonium acetate (pH6.0) (6:4). The monitoring ions for acotiamide and the internal standard were m/z 451 \rightarrow m/z 271 and m/z 465 \rightarrow m/z 364, respectively.

5.2.7. Quantification of ACh by LC-MS/MS

For the quantification of ACh, 20 μ l of stomach homogenate sample was mixed with 100 μ l of acetonitrile, and 10 μ l of internal standard was then added to the resulting

solution. After centrifugation for 10 min ($16,000 \times g$), the supernatant was collected and subjected to LC-MS/MS.

LC-MS/MS analysis was performed on an API 4000 tandem mass spectrometer with a solvent delivery system (LC-30AD) and auto-injector (SIL-30AC) using a HILIC column (Atlantis[®] HILIC; Waters). Electrospray ionization was performed in positive-ion mode. ACh and an internal standard were quantified using the selected reaction-monitoring mode at a flow rate of 0.3 ml/min acetonitrile/10 mM ammonium formate (pH 3.0) (65:35). The monitoring ions for acetylcholine and the internal standard were m/z 146 \rightarrow m/z 87 and m/z 155 \rightarrow m/z 87, respectively.

5.2.8. PBPK/PD model

All plasma concentration data were converted to blood concentration data using Equation 2-1, as follows:

$$C_a = C_p \cdot R_{bp} \dots\dots\dots 2-1$$

where C_a , C_p , and R_{bp} denote the arterial blood concentration, plasma concentration, and blood-to-plasma concentration ratio ($R_{bp}=0.84$), respectively.

The blood concentrations of acotiamide were fitted to Equation 2-2, as follows:

$$C_1 = \frac{D \cdot (\alpha - k_2)}{V_1 \cdot (\alpha - \beta)} \cdot e^{-\alpha t} + \frac{D \cdot (k_2 - \beta)}{V_1 \cdot (\alpha - \beta)} \cdot e^{-\beta t} \dots\dots\dots 2-2$$

The tissue concentrations of acotiamide were analyzed by the model shown in Fig. 3-1.

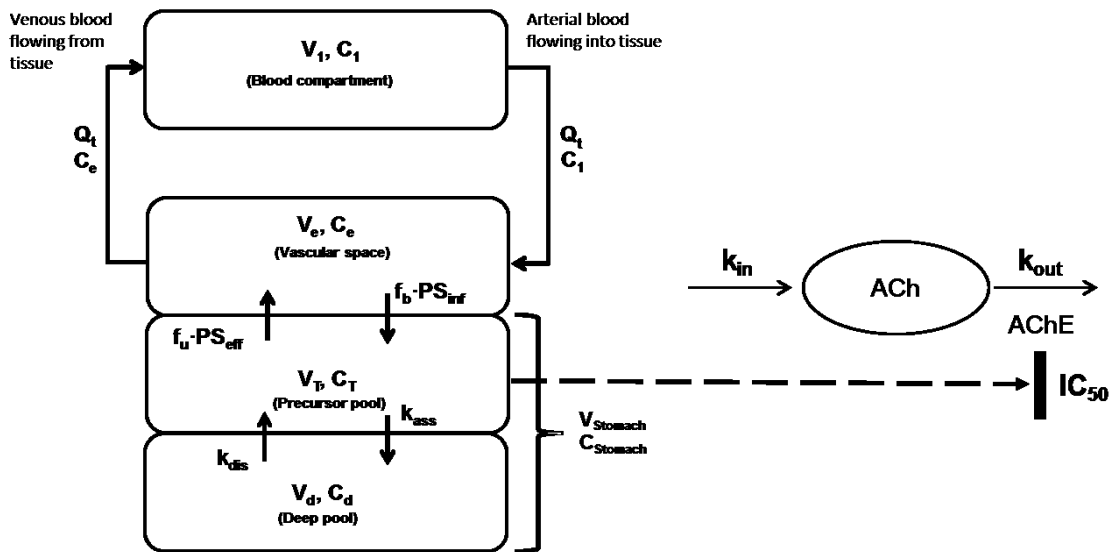


Fig. 3-1. Physiologically-based pharmacokinetic and pharmacodynamic model to describe the distribution of acotiamide and AChE inhibition in rat stomach following intravenous administration
 All terms and mass balance for the model are described in “Materials and Methods”.

The mass balance equations of each compartment are as follows:

Vascular space:

$$V_e \cdot \frac{dC_e}{dt} = Q_t \cdot (C_1 - C_e) - f_b \cdot PS_{inf} \cdot C_e + f_u \cdot PS_{eff} \cdot C_T \dots\dots\dots 2-3$$

Precursor pool:

$$V_T \cdot \frac{dC_T}{dt} = f_b \cdot PS_{inf} \cdot C_e + V_d \cdot C_d \cdot k_{dis} - f_u \cdot PS_{eff} \cdot C_T - V_T \cdot C_T \cdot k_{ass} \dots\dots\dots 2-4$$

Deep pool:

$$V_d \cdot \frac{dC_d}{dt} = V_T \cdot C_T \cdot k_{ass} - V_d \cdot C_d \cdot k_{dis} \dots\dots\dots 2-5$$

V_d , $V_{stomach}$ and $C_{stomach}$ are defined by the following equations:

$$V_d = V_T \cdot \frac{k_{ass}}{k_{dis}} \dots\dots\dots 2-6$$

$$V_{stomach} = V_T + V_d \dots\dots\dots 2-7$$

$$C_{stomach} = \frac{A_T + A_d}{V_{stomach}} \dots\dots\dots 2-8$$

where A_T and A_d denote the amounts of acotiamide in the precursor and deep pools, respectively; C_1 , C_e , C_T , and C_d denote the acotiamide concentrations in the arterial blood, vascular space, precursor pool, and deep pool, respectively; and V_e , V_T , and V_d denote the volumes of the vascular space, precursor pool, and deep pool, respectively. Q_t and $V_{stomach}$ represent blood flow rate and stomach tissue volume, respectively. $f_b \cdot PS_{inf}$ and $f_u \cdot PS_{eff}$ are the permeation clearances for the influx and efflux of acotiamide between the vascular space and precursor pool, respectively. The deep pool operates under linear conditions and can be characterized by first-order rate constants (k_{ass} and k_{dis}). V_e can be described as the product of V_i and tissue weight [33]. Data fitting of the model equations was performed using the Phoenix model of the WinNonlin version 6.1 (Pharsight Corp., Mountain View, CA, USA).

ACh concentration in the stomach was simulated using the following model. A pharmacodynamic (PD) model was used as Model 2 [43, 44], and integrated into the PBPK model to estimate the stomach distribution of ACh. According to Model 2, the rate of change in drug response can be described as follows:

$$\frac{dR}{dt} = k_{in} - k_{out} \cdot \left(1 - \frac{C_T}{IC_{50} + C_T} \right) \cdot R \dots\dots\dots 2-9$$

where k_{in} is the zero-order constant for the production of ACh, and k_{out} defines the first-order rate constant of hydrolysis of ACh by AChE. R is the observed concentration of ACh, and IC_{50} is the acotiamide concentration that produces 50% maximal effect. Data fitting of the model equations was performed using the Phoenix model of the WinNonlin version 6.1.

5.3. Results

5.3.1. PBPK modeling

Upon modeling of the disposition of acotiamide in rats, the blood and stomach concentrations of acotiamide were determined after the intravenous administration of acotiamide to rats (Fig. 3-2). The gastric concentration of acotiamide in the first two sampling point was approximately equal, suggesting the involvement of the time-consuming process in the distribution of acotiamide into the stomach. The assumption was supported by the result of integration plot analysis in the report, which showed that the distribution of acotiamide in the stomach consisted of both rapid and slow equilibrium with the blood [20]. We therefore assumed that the vascular space was involved in rapid equilibrium with the blood and the extravascular compartment was involved in slow equilibrium with the blood (Fig. 3-1). Moreover, the blood-flow independent membrane permeability clearance ($f_b \cdot PS_{inf}$) reported in the report [20], which suggested that carrier mediated uptake process was involved in the distribution of acotiamide to the stomach, was applied to the distribution process of acotiamide into the stomach. After the distribution process, acotiamide was eliminated from the blood and stomach in a biexponential manner (Fig. 3-2). Acotiamide in the stomach was slowly eliminated compared with the blood compartment (Fig. 3-2). We assumed the precursor pool where acotiamide is unbound and the deep pool where acotiamide nonspecifically interacts with cellular components (Fig. 3-1). Overall, acotiamide is first distributed into the vascular space, and subsequently transported from the vascular space to the precursor pool in the PBPK model.

5.3.2. Analysis of blood and stomach concentrations of acotiamide

The blood and stomach concentrations were fitted to a PBPK model describing the time course of acotiamide concentration in the blood and stomach (Fig. 3-2). The concentration of acotiamide in the precursor pool of stomach decreased to approximately 2 μM at 2 h after administration. The concentration of acotiamide in the deep pool of stomach was estimated below 0.01 μM after the administration of acotiamide. The terminal phase for the stomach concentration was well fitted by the deep pool of stomach. The kinetic parameters for acotiamide are summarized in Table 3-1. The fitting quality or suitability of the PBPK model was assessed using the maximized log-likelihood function (Loglik) and Akaike's information criterion (AIC), which indicated that the developed PBPK model is appropriate for describing the kinetics of acotiamide (Fig. 3-2 and Table 3-2).

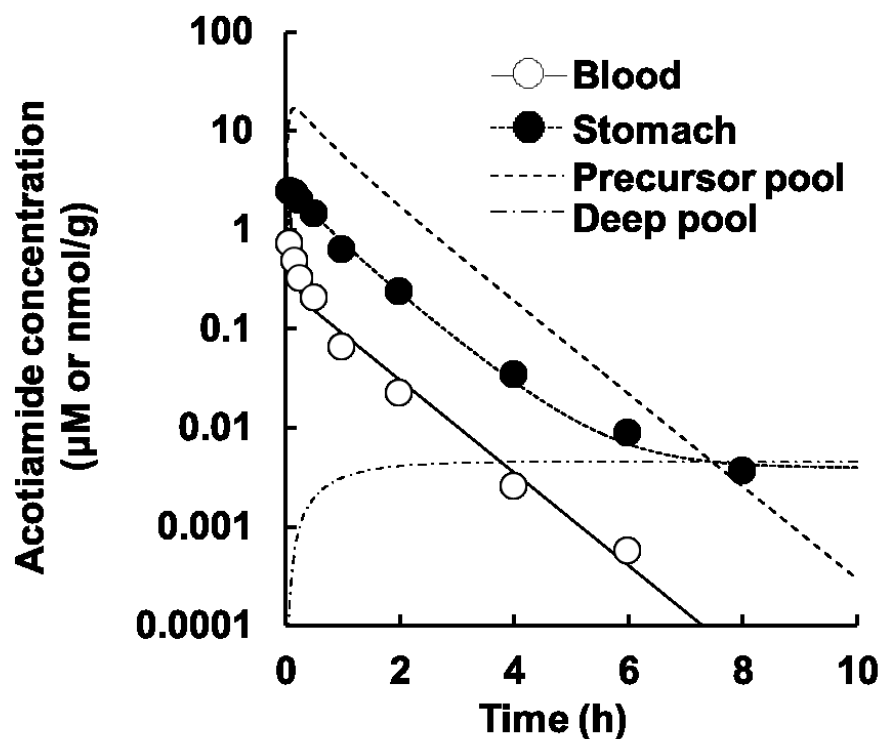


Fig. 3-2. Profiles and model simulations of acotiamide concentrations in the blood, stomach, precursor pool, and deep pool after intravenous administration to rats.

Each point and vertical bar represents the mean \pm S.E. of six rats. All values of S.E. are inside the symbols. Open and closed circles indicate blood concentration and stomach concentration, respectively. Solid, dotted, dashed, and dashed-dotted lines represent the time course of acotiamide concentration in the blood, stomach, precursor pool, and deep pool, respectively. Symbols represent experimentally observed concentrations; lines are simulated concentration profiles using the PBPK model from Fig.

3-1.

Table 3-1. Physiological and pharmacokinetic parameters for PBPK analysis in rats

| Parameter | Value | Source |
|--|------------|---|
| V_1 (ml/kg) | 302 | By fitting |
| k_1 (min^{-1}) | 0.126 | By fitting |
| k_2 (min^{-1}) | 0.0313 | By fitting |
| CL_{tot} (ml/min/kg) | 56.9 | By fitting |
| V_e (ml) | 0.441 | Calculated from V_i [20] and tissue weight [33] |
| V_{stomach} (ml) | 1.1 | Hosseini-Yeganeh and McLachlan [33] |
| $f_b \cdot PS_{\text{inf}}$ (ml/min) | 0.174 | Yoshii <i>et al.</i> , 2011 [20] |
| Q_t (ml/min) | 1.1 | Hosseini-Yeganeh and McLachlan [33] |
| V_T (ml) | 0.133 | By fitting |
| $f_u \cdot PS_{\text{eff}}$ (ml/min) | 0.00600 | By fitting |
| k_{ass} (min^{-1}) | 0.0000320 | By fitting |
| k_{dis} (min^{-1}) | 0.00000485 | By fitting |
| IC_{50} (μM) | 1.79 | <i>In vitro</i> study |
| k_{in} (nmol/g of tissue/min) | 0.00314 | By fitting |
| k_{out} (min^{-1}) | 0.00415 | By fitting |

Table 3-2. Fitting quality of the PBPK model for the time course of acotiamide concentrations in blood and stomach

| Loglik | AIC |
|--------|-------|
| 36.0 | -61.9 |

Loglik, maximized log-likelihood function; AIC, Akaike's information criterion

Calculated using number of observations=26 and number of parameters=5

5.3.3. Inhibition of the hydrolysis of MATP+ by acotiamide

The effect of acotiamide on AChE derived from rat stomach is shown in Fig. 3-3. The hydrolysis velocity of MATP+ decreased with increasing acotiamide concentration, with an IC_{50} value of $1.79 \mu\text{M}$ (Table 3-1).

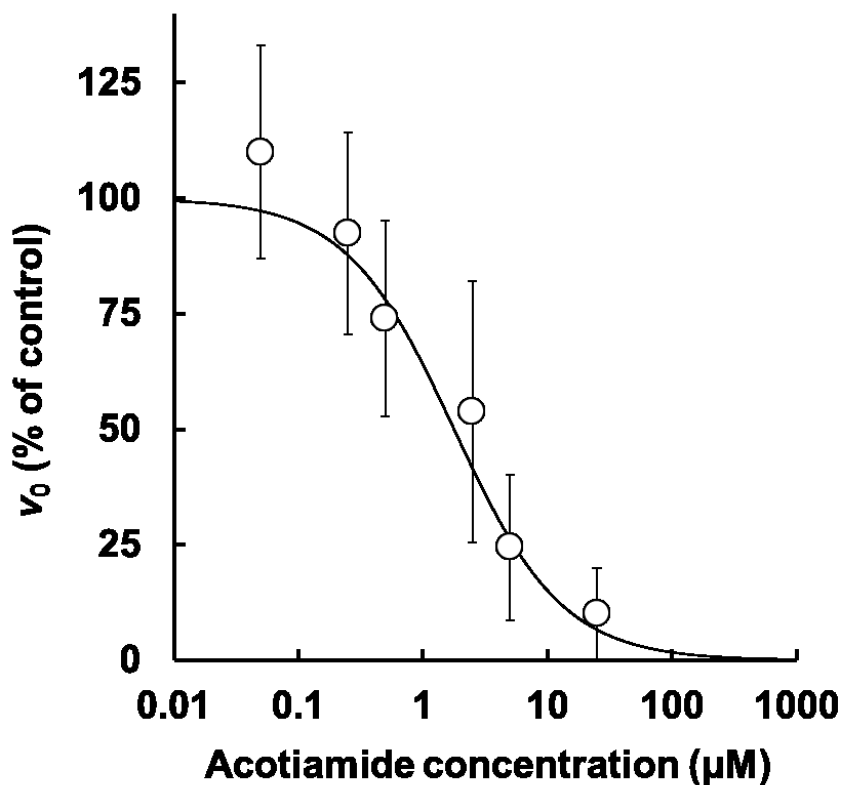


Fig. 3-3. Inhibition of MATP+ hydrolysis by acotiamide.

Each point and vertical bar showing the hydrolysis velocity (v_0) of MATP+ represents the mean \pm S.E. for three determinations.

5.3.4. PD modeling

The indirect response model was linked with the PBPK model for describing the inhibition of AChE by acotiamide. The concentration of acotiamide used in the PD model was chosen as the concentration of acotiamide in the precursor pool of stomach, which covered the IC_{50} value for the inhibition of AChE by acotiamide.

5.3.5. Analysis of stomach concentration of ACh

The profile of ACh after the administration of acotiamide is shown in Fig. 3-4. The concentration of ACh rose to 131% (% of baseline) at 2 h after administration of acotiamide. When the data of ACh concentrations was fitted to the PBPK/PD model without fixing the PD parameters (k_{in} , k_{out} and IC_{50}), k_{in} , k_{out} and IC_{50} were 0.00337 nmol/g of tissue/min, 0.00446 min^{-1} and 2.10 μM , respectively. At that fitting, Loglik and AIC were 43.9 and -75.8, respectively, which indicated that the PBPK/PD model is appropriate for describing the kinetics of ACh. When the data of ACh concentrations was fitted to the model with fixing IC_{50} (1.79 μM), the profile of stomach concentration of ACh was well estimated by the PBPK/PD model on the assumption that acotiamide in the precursor pool of stomach inhibited AChE (Fig. 3-4).

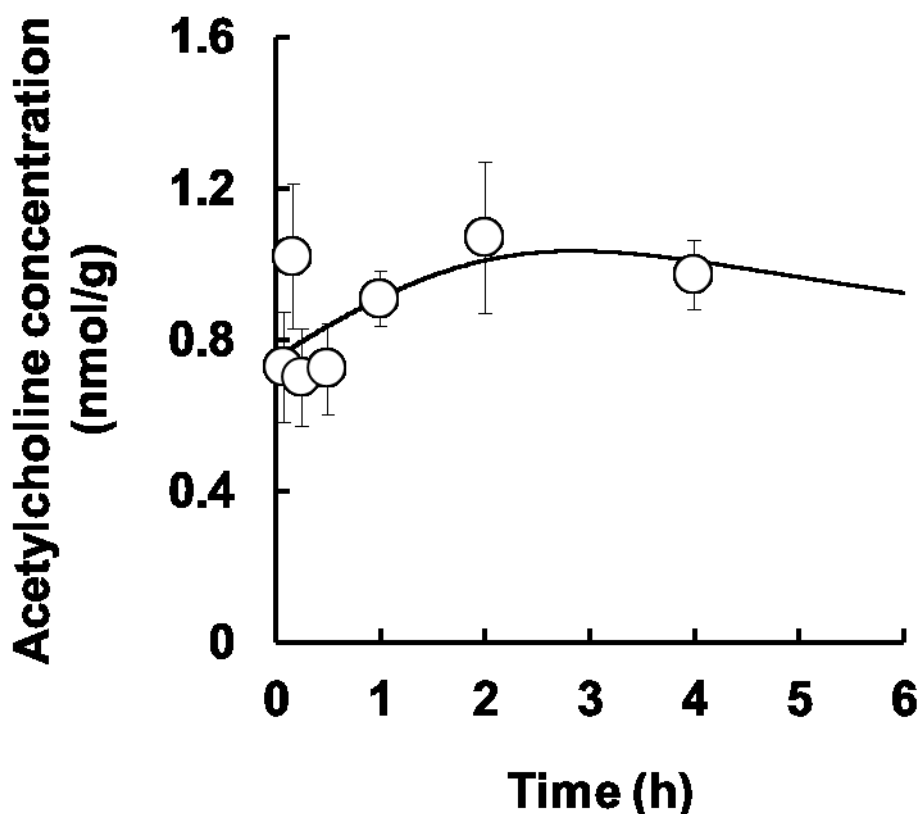


Fig. 3-4. Profile and model simulation of ACh concentration in the stomach homogenate after intravenous administration of acotiamide to rats.

Each point and vertical bar represents the mean \pm S.E. of six rats. Symbols represent experimentally observed concentrations, while curves show the simulated concentration profiles from the PBPK/PD model (Fig. 3-1).

5.4. Discussion

The stomach concentration of acotiamide was higher than the blood concentration in the first time point when acotiamide concentration was measured after intravenous administration of acotiamide to rats. Acotiamide was slowly eliminated in the stomach compared to the blood. The PBPK model well described the profile of acotiamide concentration in the blood and stomach in the assumption that acotiamide was rapidly distributed into the vascular space, uptaken to the precursor pool of stomach by carrier mediated process and permeated in the deep pool of stomach. ACh, which was determined as the marker of the involvement of acotiamide in inhibiting AChE, reached the maximum concentration in the stomach at 2 h after intravenous administration of acotiamide, while the stomach concentration of acotiamide peaked at 0.0833 h, indicating the existence of time lag between the stomach concentration of acotiamide and ACh. The unbound concentration of acotiamide in the precursor pool was higher than the *in vitro* IC₅₀ value of acotiamide for inhibiting AChE activity by approximately 2 h after administration of acotiamide. The PD model well described the profile of ACh concentration in the stomach in the assumption that the unbound concentration of acotiamide in the precursor pool inhibited AChE with the *in vitro* IC₅₀ for AChE inhibition. These results suggested that acotiamide inhibited AChE in the precursor pool of stomach where acotiamide was distributed by carrier mediated process.

No reports have been published on a PK model for the distribution of drugs from blood to stomach as the pharmacological target although some reports have been reported on a PK model containing stomach as delivery organ of drugs to small intestine [45,46,47].

The precursor and deep pool of stomach were put in the model to describe the rate-limiting step in the uptake of acotiamide by stomach and slower elimination of acotiamide from stomach than blood. Acotiamide in the precursor pool of stomach plays an important role in the elevation of ACh in the stomach though the anatomical meanings of these compartments remain unclear. It's normally difficult to estimate the microenvironmental concentration of drugs in tissue. For brain, microdialysis method was applied to estimate the unbound concentration of drugs penetrating into brain [48,49]. The method for prediction of the unbound concentration of drugs in brain was also reported by Fridén *et al* [50]. For stomach, the application of microdialysis to submucosa which is thicker than muscular layer and unrelated with gastric motility in the gastric layers was only reported [51,52]. Moreover, there is no report concerning the method for prediction of the unbound concentration of drugs in stomach. Thus, we proposed a mechanism based PK model to estimate the concentration of drugs exerting their pharmacological effects in tissues like gastroprokinetic agents in stomach.

The selectivity of drug to its target is achieved by the specific affinity to drug targets, the selective access to site where drug targets exist, and/or the unique localization of drug target. For example, histamine H₂ receptor, which is only involved in the regulation of gastric acid secretion among four subtypes of histamine H receptor, is a selective target for the suppressor of gastric acid secretion [53,54]. L-type amino acid transporter 1 is considered as a specific target for antitumor because L-type amino acid transporter 1, transporting amino acids needed for the growth of cancer cells, selectively expresses in cancer cells [55,56]. AChE, the target of acotiamide is a ubiquitous enzyme. In addition, ACh which is regulated by AChE interacts with each subtype of muscarinic receptor. There might be no selectivity on the pathway from the contact of acotiamide with AChE to the evoking of pharmacological action, so the selectivity of acotiamide to its target

might be derived only from the feature in the distribution of acotiamide. Thus, it's seems important to put in the distribution parameters to stomach in the development of the PBPK/PD model. $f_b \cdot PS_{inf}$ of the distribution parameters was calculated from the uptake clearance of acotiamide to stomach [20]. The uptake clearance can be expressed as the slope in the integration plot, where stomach to blood concentration ratio is plotted against area under the blood concentration curve to blood concentration ratio when the uptake of acotiamide was determined in a short time, during which the efflux and/or elimination of acotiamide from stomach were negligible. V_e of the distribution parameters (0.401 ml/g of tissue) was calculated as the product of the intercept (V_i) of y axis of integration plot and tissue weight ($V_i \cdot \text{tissue weight}$). When V_e was compared with the volume of capillary bed (0.0108 ml/g of tissue) [57] and inulin space (0.295 ml/g of tissue) [20], V_e was similar to inulin space, an extracellular space. Therefore, $f_b \cdot PS_{inf}$ might represent the transport of acotiamide through plasma membrane of gastric cells. Moreover, the volume of precursor pool (V_T) which was 12.1% of the volume of stomach ($V_{stomach}$) was similar to fraction of acotiamide distributed to the stomach cytosol (12.0%) reported in previous report [20]. The result suggested that the volume of precursor and deep pool reflected fraction of acotiamide distributed to cytosol and organelle of gastric cells, respectively.

The time lag between drug concentration and the effect was often observed [43,44,58]. For describing the delay of drug effect, the PD models like hypothetical effect compartment model and indirect response model were used. The hypothetical effect compartment model is useful in the case that mechanism of the delay for drug effect is unknown, while the indirect response model is available for drugs whose mechanism of the delay is derived from the mechanism of action. An indirect response model was chosen as the PD model because acotiamide is a known AChE inhibitor. Dayneka *et al.* classified the indirect response model into four models types-based on the mechanism of

action [43]. Based on this classification, the effects of reversible anticholinesterase agents, which inhibit the enzymatic breakdown of ACh, demonstrated that the model could be categorized as Model 2. The rate of change in drug response using this model is described by Equation 2-9, and many drugs described in this manner show a delay compared to the time course of the drug concentration. Jusko *et al.* used an indirect response model to describe the muscular response as ACh level in patients with myasthenia gravis during therapy using pyridostigmine, acetylcholinesterase inhibitor [59]. Therefore, the indirect response model is suitable for describing the inhibitory effect of acotiamide on AChE in rat stomach.

Normally, acetylthiocholine (ATCh) is used to evaluate AChE activity [60]. However, ATCh is a known substrate of both AChE and butyrylcholinesterase (BChE), meaning BChE inhibitors such as iso-OMPA need to be included in the incubation medium when investigating acotiamide effects [15]. Recently, Kikuchi *et al.* reported that MATP⁺ was suitable AChE selective substrates for detecting of AChE activity [42]. Therefore, in this study, we used MATP⁺ as substrate of AChE for investigation of the effects of acotiamide on the AChE activity. Hydrolysis velocity of MATP⁺ was decreased by the addition of acotiamide, with the IC₅₀ value of 1.79 μM. Kawachi *et al.* have reported that acotiamide inhibited ATCh hydrolysis by stomach homogenate with IC₅₀ value of 2.3 μM [17]. Furthermore, acotiamide also inhibited human AChE with K_i value of 0.61 μM [15]. The observation was similar to these previously results, therefore, it was considered that using of MATP⁺ for investigation of AChE inhibition is appropriate.

In conclusion, we elucidated the relationship of the blood and stomach concentration of acotiamide with the pharmacological action. Acotiamide was distributed by carrier mediated process and inhibited AChE in the precursor pool of stomach. Acotiamide in the precursor pool plays an important role for producing the pharmacologic action. Moreover,

we proposed PBPK/PD model to describe the pharmacologic action of acotiamide in stomach.

5.5. Summary

Acotiamide, a gastroprokinetic agent used to treat FD, is transported to at least two compartments in rat stomach. However, the role of these stomach compartments in pharmacokinetics and pharmacodynamics of acotiamide remains unclear. Thus, the purpose of this study was to elucidate the relationship of the blood and stomach concentration of acotiamide with its inhibitory effect on AChE.

Concentration profiles of acotiamide and ACh were determined after intravenous administration to rats and analyzed by PBPK/PD model containing vascular space, precursor pool and deep pool of stomach.

Acotiamide was eliminated from the blood and stomach in a biexponential manner. The PBPK/PD model estimated that acotiamide concentration in the precursor pool exceeded 2 μM at approximately 2 h after administration. Acotiamide inhibited AChE activity *in vitro* with a 50% inhibitory concentration of 1.79 μM . ACh reached the maximum concentration at 2 h after administration.

The PBPK/PD model well described the profile of acotiamide and ACh concentration in the stomach in the assumption that acotiamide was distributed by carrier mediated process and inhibited AChE in the precursor pool of stomach. Thus, Acotiamide in the precursor pool plays an important role for producing the pharmacological action.

6. Conclusion

Acotiamide is an AChE inhibitor and gastroprokinetic agent. There is no report for the severe adverse effects like cholinergic crisis and fasciculation by inhibition of cholinergic nerves in brain and skeletal muscle, so acotiamide might have selectivity for stomach. AChE is ubiquitously located in organs other than stomach. The selectivity of acotiamide to stomach may be derived from the selective distribution of acotiamide to stomach. The distribution of acotiamide to stomach and other organs is related with the pharmacological and adverse effect of acotiamide, respectively. Therefore, studies on the distribution of acotiamide are important to understand the pharmacological and adverse effects of acotiamide. To elucidate the distribution of acotiamide to tissues/organs, the following studies were performed.

To examine whether the concentration of acotiamide at the site of action is sufficient to inhibit AChE, the distribution of [^{14}C]acotiamide around nerve cells in the *myenteric plexus* of rat and dog stomachs. AChE activity staining showed that AChE as target of acotiamide was located around nerve cells in the *myenteric plexus* of rat and dog stomachs. The macro-autoradiography showed the concentration of radioactivity was 27.9 μM in rat stomach, which was 12 times higher than IC_{50} of acotiamide for rat AChE. Being different from rats, the distribution of radioactivity in the muscular layer was distinguishable from that in the mucosal layer in dog stomach. The concentration of radioactivity in the muscular layer of dog stomach (1.41 μM) was approximately two-times lower than those in the mucosal layer, however, it was approximately 1.2 times higher than IC_{50} of acotiamide for dog AChE. The results of micro-autoradiography also showed the radioactivity distributed homogenously in the muscular layer of rat stomach, suggesting the concentration of radioactivity around the ganglion of *myenteric plexus* is similar to that

in the muscular layer of stomach. These findings suggest acotiamide distributes to the *myenteric plexus* of stomach, a putative site of acotiamide action, with adequate concentrations to inhibit AChE, in both of rat and dog stomachs.

To reveal the mechanism of distribution of acotiamide from blood to stomach, the tissue distribution of acotiamide was investigated in rats. The tissue-to-plasma concentration ratio ($K_{p,app,in vivo}$) for stomach decreased from 4.1 to 2.4 ml/g of tissue at steady state with increasing plasma concentrations, whereas the $K_{p,app,in vivo}$ for skeletal muscle was much lower and constant regardless of the concentration of acotiamide in plasma. *In vitro* binding to stomach tissue protein exhibited a linear profile, with a predicted $K_{p,app,in vitro}$ of 2.2 from free fractions under linear conditions. Therefore, protein binding to stomach tissue might only play a limited role in the stomach distribution of acotiamide. The influx permeability ($f_{u,b} \cdot PS_{inf,app}$) in the stomach exhibited dose-dependent saturation at the lowest range of examined blood unbound concentrations of acotiamide, whereas that in skeletal muscle exhibited only minimal dose dependence. In addition, the unbound concentration ratio of stomach to plasma (2.8) at steady state was markedly higher than unity. Taken together, these results suggest that carrier-mediated concentrative uptake processes play an important role in the distribution of acotiamide to the stomach, but not skeletal muscle.

To elucidate a role of carrier-mediated concentrative uptake process on the pharmacokinetics and pharmacodynamics of acotiamide, concentration profiles of acotiamide and ACh were determined after intravenous administration to rats and analyzed by PBPK/PD model. The PBPK/PD model was developed in the assumption that acotiamide was distributed by carrier mediated process and increase ACh via inhibition of AChE. Since acotiamide was eliminated from the blood and stomach in a biexponential manner, compartments equilibrated rapidly and slowly with blood were set to the

PBPK/PD model. As the elimination of acotiamide from stomach was slower than that from blood, the precursor and deep pool of stomach was built in PBPK/PD model. The PBPK/PD model estimated that acotiamide concentration in the precursor pool exceeded 2 μM at approximately 2 h after administration. Acotiamide inhibited AChE activity *in vitro* with IC_{50} of 1.79 μM . ACh reached the maximum concentration at 2 h after administration. The PBPK/PD model well described the profile of acotiamide and ACh concentration in the stomach. Thus, the carrier-mediated concentrative uptake process plays an important role for pharmacokinetics and pharmacodynamics of acotiamide.

These studies suggest that acotiamide is distributed via carrier-mediated concentrative uptake process to stomach, inhibits AChE around nerve cells in the *myenteric plexus* of stomach, and increases ACh involving gastric motility, while acotiamide is hardly ever distributed to brain and skeletal muscle. Therefore, acotiamide has effectiveness and safety for the treatment of FD.

Further studies are needed for the identification of transporter involved in the carrier-mediated concentrative uptake process of acotiamide to stomach.

7. References

- 1 Tack J, Talley NJ (2013) Functional dyspepsia--symptoms, definitions and validity of the Rome III criteria, *Nat. Rev. Gastroenterol. Hepatol.* 10:134-41.
- 2 Talley NJ, Axon A, Bytzer P, Holtmann G, Lam SK, Van Zanten S (1998) Management of uninvestigated and functional dyspepsia: a Working Party report for the World Congresses of Gastroenterology 1998. *Aliment Pharmacol Ther.* 13:1135-48.
- 3 Tack J, Masaoka T, Janssen P (2011) Functional dyspepsia. *Curr Opin Gastroenterol.* 27:549-57.
- 4 Kamino D, Manabe N, Hata J, Haruma K, Tanaka S, Chayama K (2008) Long-term Ultrasonographic Follow-up Study of Gastric Motility in Patients with Functional Dyspepsia, *J. Clin. Biochem. Nutr.* 42:144-149.
- 5 Quigley EM (2004) Review article: gastric emptying in functional gastrointestinal disorders, *Aliment. Pharmacol. Ther.* 20:56-60.
- 6 Maurer AH (2012) Advancing gastric emptying studies: standardization and new parameters to assess gastric motility and function, *Semin. Nucl. Med.* 42:101-12.
- 7 Read NW, Houghton LA (1989) Physiology of gastric emptying and pathophysiology of gastroparesis, *Gastroenterol. Clin. North. Am.* 18:359-73.
- 8 Mizuta Y, Shikuwa S, Isomoto H, Mishima R, Akazawa Y, Masuda J, *et al.* (2006) Recent insights into digestive motility in functional dyspepsia. *J Gastroenterol.* 41:1025-1040.
- 9 Tack J (2008) Prokinetics and fundic relaxants in upper functional GI disorders. *Curr Opin Pharmacol.* 8:690-696.

- 10 Sun Y, Song G, McCallum RW (2013) Evaluation of acotiamide for the treatment of functional dyspepsia, *Expert. Opin. Drug. Metab. Toxicol.* 31:1-8.
- 11 Kusunoki H, Haruma K, Manabe N, Imamura H, Kamada T, Shiotani A, *et al.* (2012) Therapeutic efficacy of acotiamide in patients with functional dyspepsia based on enhanced postprandial gastric accommodation and emptying: randomized controlled study evaluation by real-time ultrasonography, *Neurogastroenterol. Motil.* 24:540-5.
- 12 Matsueda K, Hongo M, Tack J, Saito Y, Kato H (2012) A placebo-controlled trial of acotiamide for meal-related symptoms of functional dyspepsia, *Gut* 61:821-8.
- 13 Nolan ML, Scott LJ (2013) Acotiamide: first global approval. *Drugs.* 73:1377-83.
- 14 Sun Y, Song G, McCallum RW (2014) Evaluation of acotiamide for the treatment of functional dyspepsia. *Expert Opin Drug Metab Toxicol.* 10:1161-8.
- 15 Matsunaga Y, Tanaka T, Yoshinaga K, Ueki S, Hori Y, Eta R, *et al.* (2011) Acotiamide hydrochloride (Z-338), a new selective acetylcholinesterase inhibitor, enhances gastric motility without prolonging QT interval in dogs: comparison with cisapride, itopride, and mosapride, *J. Pharmacol. Exp. Ther.* 336:791-800.
- 16 Matsunaga Y, Ueki S, Matsumura T, Nomura Y, Yoneta T, Kurimoto T, *et al.* (1998) Z-338, a novel gastroprokinetic agent stimulates gastrointestinal motor activity and improves delayed gastric emptying in the dog and rat. *Jpn J Pharmacol* 76(suppl. 1):290.
- 17 Kawachi M, Matsunaga Y, Tanaka T, Hori Y, Ito K, Nagahama K, *et al.* (2011) Acotiamide hydrochloride (Z-338) enhances gastric motility and emptying by inhibiting acetylcholinesterase activity in rats, *Eur. J. Pharmacol.* 666:218-225.
- 18 Romi F, Gilhus NE, Aarli JA (2005) Myasthenia gravis: clinical, immunological, and therapeutic advances. *Acta Neurol Scand* 111:134–141.

- 19 Zheng HL, Hu YM, Bao JJ, Xu JM (2010) Transfer and distribution of amoxicillin in the rat gastric mucosa and gastric juice and the effects of rabeprazole. *Acta Pharmacol Sin* 31:501–508.
- 20 Yoshii K, Hirayama M, Nakamura T, Toda R, Hasegawa J, Takei M, *et al.* (2011) Mechanism for distribution of acotiamide, a novel gastrokinetic agent for the treatment of functional dyspepsia, in rat stomach, *J. Pharm. Sci.* 100:4965-4973.
- 21 Furness JB, Callaghan BP, Rivera LR, Cho HJ (2014) The enteric nervous system and gastrointestinal innervation: integrated local and central control, *Adv. Exp. Med. Biol.* 817:39-71.
- 22 Maas J, Binder R, Steinke W (2000) Quantitative whole-body autoradiography: recommendations for the standardization of the method, *Regul Toxicol Pharmacol.* 31:S15-21.
- 23 Binder R, Archimbaud Y (2000) Sensitivity of radioluminography using (14)C-labeled tracers in whole-body sections of rats, *Regul Toxicol Pharmacol.* 31:S23-6.
- 24 Ubukata K, Nakayama A, Mihara R (2011) Pharmacokinetics and metabolism of N-[N-[3-(3-hydroxy-4-methoxyphenyl) propyl]- α -aspartyl]-L-phenylalanine 1-methyl ester, monohydrate (advantame) in the rat, dog, and man, *Food Chem Toxicol.* 49:Suppl 1:S8-29.
- 25 Woodburn KW, Fong KL, Wilson SD, Sloneker S, Strzemienski P, Solon E, *et al.* (2013) Peginesatide clearance, distribution, metabolism, and excretion in monkeys following intravenous administration, *Drug Metab Dispos.* 41:774-84.
- 26 Nagahama K, Matsunaga Y, Kawachi M, Ito K, Tanaka T, Hori Y, *et al.* (2012) Acotiamide, a new orally active acetylcholinesterase inhibitor, stimulates

- gastrointestinal motor activity in conscious dogs, *Neurogastroenterol. Motil.* 24:566-74.
- 27 Kyösola K, Rechart L, Veijola L, Waris T, Penttilä O (1980) Innervation of the human gastric wall, *J. Anat.* 131:453-70.
- 28 Summerfield SG, Read K, Begley DJ, Obradovic T, Hidalgo IJ, Coggon S, *et al.* (2007) Central nervous system drug disposition: the relationship between in situ brain permeability and brain free fraction. *J Pharmacol Exp Ther* 322:205–213.
- 29 Kim DC, Sugiyama Y, Satoh H, Fuwa T, Iga T, Hanano M (1988) Kinetic analysis of in vivo receptor-dependent binding of human epidermal growth factor by rat tissues. *J Pharm Sci* 77:200–207.
- 30 Liu KX, Kato Y, Narukawa M, Kim DC, Hanano M, Higuchi O, *et al.* (1992) Importance of the liver in plasma clearance of hepatocyte growth factors in rats. *Am J Physiol* 263:G642–649.
- 31 Wilkinson GR, Shand DG (1975) Commentary: a physiological approach to hepatic drug clearance. *Clin Pharmacol Ther* 18:377–390.
- 32 Pang KS, Rowland M (1977) Hepatic clearance of drugs. I. Theoretical considerations of a "well-stirred" model and a "parallel tube" model. Influence of hepatic blood flow, plasma and blood cell binding, and the hepatocellular enzymatic activity on hepatic drug clearance. *J Pharmacokinet Biopharm* 5:625–653.
- 33 Hosseini-Yeganeh M, McLachlan AJ (2002) Physiologically based pharmacokinetic model for terbinafine in rats and humans. *Antimicrob Agents Chemother* 46:2219–2228.
- 34 Wierzba K, Sugiyama Y, Okudaira K, Iga T, Hanano M (1987) Tubulin as a major determinant of tissue distribution of vincristine. *J Pharm Sci* 76:872–875.

- 35 Jonker JW, Wagenaar E, Mol CA, Buitelaar M, Koepsell H, Smit JW, *et al.* (2001) Reduced hepatic uptake and intestinal excretion of organic cations in mice with a targeted disruption of the organic cation transporter 1 (Oct1 [Slc22a1]) gene. *Mol Cell Biol* 21:5471–5477.
- 36 Okuda M, Saito H, Urakami Y, Takano M, Inui K (1996) cDNA cloning and functional expression of a novel rat kidney organic cation transporter, OCT2. *Biochem Biophys Res Commun* 224:500–507.
- 37 Wang DS, Jonker JW, Kato Y, Kusuhara H, Schinkel AH, Sugiyama Y (2002) Involvement of organic cation transporter 1 in hepatic and intestinal distribution of metformin. *J Pharmacol Exp Ther* 302:510–515.
- 38 Tack J, Masclee A, Heading R, Berstad A, Piessevaux H, Popiela T, *et al.* (2009) A dose-ranging, placebo-controlled, pilot trial of Acotiamide in patients with functional dyspepsia. *Neurogastroenterol Motil* 21:272–280.
- 39 Furuta S, Kamada E, Omata T, Sugimoto T, Kawabata Y, Yonezawa K, *et al.* (2004) Drug-drug interactions of Z-338, a novel gastroprokinetic agent, with terfenadine, comparison with cisapride, and involvement of UGT1A9 and 1A8 in the human metabolism of Z-338. *Eur J Pharmacol* 497:223–231.
- 40 Grams B, Harms A, Braun S, Strassburg CP, Manns MP, Obermayer-Straub P (2000) Distribution and inducibility by 3-methylcholanthrene of family 1 UDP-glucuronosyltransferases in the rat gastrointestinal tract. *Arch Biochem Biophys* 377:255–265.
- 41 Shelby MK, Cherrington NJ, Vansell NR, Klaassen CD (2003) Tissue mRNA expression of the rat UDP-glucuronosyltransferase gene family. *Drug Metab Dispos* 31:326–333.

- 42 Kikuchi T, Okamura T, Fukushi K, Irie T (2010) Piperidine-4-methanthiol ester derivatives for a selective acetylcholinesterase assay. *Biol Pharm Bull.* 33:702-706.
- 43 Dayneka NL, Garg V, Jusko WJ (1993) Comparison of four basic models of indirect pharmacodynamic responses. *J Pharmacokinet Biopharm.* 21:457-478.
- 44 Felmlee MA, Morris ME, Mager DE (2012) Mechanism-based pharmacodynamic modeling. *Methods MolBiol.* 929:583-600.
- 45 Agoram B, Woltosz WS, Bolger MB (2001) Predicting the impact of physiological and biochemical processes on oral drug bioavailability. *Adv Drug Deliv Rev.* 50:S41-67.
- 46 Fenneteau F, Poulin P, Nekka F (2010) Physiologically based predictions of the impact of inhibition of intestinal and hepatic metabolism on human pharmacokinetics of CYP3A substrates. *J Pharm Sci.* 99:486-514.
- 47 Poulin P, Jones RD, Jones HM, Gibson CR, Rowland M, Chien JY, *et al.* (2011) PHRMA CPCDC initiative on predictive models of human pharmacokinetics, part 5: prediction of plasma concentration-time profiles in human by using the physiologically-based pharmacokinetic modeling approach. *J Pharm Sci.* 100:4127-57.
- 48 Chen X, Loryan I, Payan M, Keep RF, Smith DE, Hammarlund-Udenaes M (2014) Effect of transporter inhibition on the distribution of cefadroxil in rat brain. *Fluids Barriers CNS.* 11:25.
- 49 Sadiq MW, Boström E, Keizer R, Björkman S (2013) Hammarlund-Udenaes M. Oxymorphone active uptake at the blood-brain barrier and population modeling of its pharmacokinetic-pharmacodynamic relationship. *J Pharm Sci.* 102:3320-31.

- 50 Fridén M, Gupta A, Antonsson M, Bredberg U, Hammarlund-Udenaes M (2007) In vitro methods for estimating unbound drug concentrations in the brain interstitial and intracellular fluids. *Drug Metab Dispos.* 35:1711-9.
- 51 Ericsson P, Håkanson R, Norlén P (2010) Gastrin response to candidate messengers in intact conscious rats monitored by antrum microdialysis. *Regul Pept.* 163:24-30.
- 52 Cibicek N, Zivna H, Vrablova E, Cibicek J, Cermakova E, Palicka V (2010) Gastric submucosal microdialysis in the detection of rat stomach ischemia--a comparison of the $^3\text{H}_2\text{O}$ efflux technique with metabolic monitoring. *Physiol Meas.* 31:1355-68.
- 53 Lin TM, Evans DC, Warrick MW, Pioch RP (1986) Actions of nizatidine, a selective histamine H₂-receptor antagonist, on gastric acid secretion in dogs, rats and frogs. *J Pharmacol Exp Ther.* 239:406-10.
- 54 Schubert ML, Peura DA (2008) Control of gastric acid secretion in health and disease. *Gastroenterology.* 134:1842-60.
- 55 Kanai Y, Segawa H, Miyamoto Ki, Uchino H, Takeda E, Endou H (1998) Expression cloning and characterization of a transporter for large neutral amino acids activated by the heavy chain of 4F2 antigen (CD98). *J Biol Chem.* 273:23629-32.
- 56 Wang Q, Bailey CG, Ng C, Tiffen J, Thoeng A, Minhas V, *et al.* (2011) Androgen receptor and nutrient signaling pathways coordinate the demand for increased amino acid transport during prostate cancer progression. *Cancer Res.* 71:7525-36.
- 57 Bernareggi A, Rowland M (1991) Physiologic modeling of cyclosporin kinetics in rat and man. *J Pharmacokinet Biopharm.* 19:21-50.
- 58 Ito Y, Harada T, Fushimi K, Kagawa Y, Oka H, Nakazawa H, *et al.* (2010) Pharmacokinetic and pharmacodynamic analysis of acetylcholinesterase inhibition by distigmine bromide in rats. *Drug Metab Pharmacokinet.* 25:254-61.

- 59 Jusko WJ, Ko HC (1994) Physiologic indirect response models characterize diverse types of pharmacodynamic effects. *Clin Pharmacol Ther.* 56:406-19.
- 60 Ellman GL, Courtney KD, Andres V Jr, Feather-Stone RM (1961) A new and rapid colorimetric determination of acetylcholinesterase activity. *Biochem Pharmacol* 7:88-95.

8. Papers in publication

This thesis is comprised of the following published papers:

1. Yoshii K, Yamaguchi T, Hirayama M, Toda R, Kinomoto T, Kawabata Y, Chiba K. (2016) Distribution of acotiamide, an orally active acetylcholinesterase inhibitor, into the myenteric plexus of rat and dog stomachs. *Life Sci* 145: 93–97. doi:10.1016/j.lfs.2015.12.020.
2. Yoshii K, Hirayama M, Nakamura T, Toda R, Hasegawa J, Takei M, Mera Y, Kawabata Y. (2011) Mechanism for distribution of acotiamide, a novel gastroprokinetic agent for the treatment of functional dyspepsia, in rat stomach, *J. Pharm. Sci.* 100:4965-4973. doi: 10.1002/jps.22649.
3. Yoshii K, Iikura M, Hirayama M, Toda R, Kawabata Y. (2016) Physiologically-based pharmacokinetic and pharmacodynamic modeling for the inhibition of acetylcholinesterase by acotiamide, a novel gastroprokinetic agent for the treatment of functional dyspepsia, in rat stomach. *Pharm Res* 33: 292-300. doi: 10.1007/s11095-015-1787-y.

9. Acknowledgements

The author would like to express his sincere appreciation to Prof. Dr. Kan Chiba, Department of Pharmacology & Toxicology, Graduate School of Pharmaceutical Sciences, Chiba University, who offered invaluable guidance, thoughtful discussions, and continuous support throughout the work on this thesis.

Special thanks are also extended to Prof. Dr. Toshihiko Toida, Department of Clinical and Analytical Biochemistry, Graduate School of Pharmaceutical Sciences, Chiba University, Prof. Dr. Akihiro Hisaka, Department of Clinical Pharmacology and Pharmacometrics, Graduate School of Pharmaceutical Sciences, Chiba University, Prof. Dr. Naoto Yamaguchi, Department of Molecular Cell Biology, Graduate School of Pharmaceutical Sciences, Chiba University, and Prof. Dr. Kousei Ito, Department of Biopharmaceutics, Graduate School of Pharmaceutical Sciences, Chiba University for their reviewing this thesis.

This research has been carried out in Toxicology & Pharmacokinetics Research, ZERIA Pharmaceutical Co., Ltd. The author wishes to express his gratitude to Sachiaki Ibe, Chairman & CEO of ZERIA Pharmaceutical Co., Ltd, as well as Mitsuaki Ibe, President & COO, Dr. Mikio Kan, Advisor, Dr. Hiroki Kato, Director and Dr. Yoshihiro Hiraga, Director for giving him the opportunity to work on the research and providing positive support.

The author is especially grateful to Dr. Yoshihiro Kawabata, Manager of Toxicology & Pharmacokinetics Research who provided many constructive discussions, professional guidance, and continuous encouragement for him to proceed on the research and publications. The author also wishes to thank Ryoko Toda, Masamichi Hirayama, Minami Iikura, Toshifumi Nakamura, Junko Hasegawa, Takashi Yamaguchi and Toshiko

Kinomoto for their contributions in this work. The author is also thankful to Dr. Yukinori Mera, previous Manager of Toxicology & Pharmacokinetics Research and Dr. Mineo Takei, Manager of Research Planning & Coordination, for their knowledge and assistance.

Finally, the author also expresses sincere thanks to his wife for her support and encouragement.

10. Reviewers

The thesis was reviewed by the following members of thesis committee who were designated by the Graduate School of Pharmaceutical Sciences, Chiba University.

| | | |
|----------------|------------------------|--|
| Chief reviewer | Kan Chiba, Ph.D. | Professor of Graduate School of Pharmaceutical Sciences, Chiba University |
| Reviewer | Toshihiko Toida, Ph.D. | Professor of Graduate School of Pharmaceutical Sciences, Chiba University |
| Reviewer | Naoto Yamaguchi, Ph.D. | Professor of Graduate School of Pharmaceutical Sciences, Chiba University |
| Reviewer | Akihiro Hisaka, Ph.D. | Professor of Graduate School of Pharmaceutical Sciences, Chiba University |
| Reviewer | Kousei Ito, Ph.D. | Professor of Graduate School of Pharmaceutical Sciences, Chiba University |